

High-pressure Processing: Kinetic Models for Microbial and Enzyme Inactivation

The Faculty of Oregon State University has made this article openly available.
Please share how this access benefits you. Your story matters.

Citation	Serment-Moreno, V., Barbosa-Cánovas, G., Torres, J. A., & Welti-Chanes, J. (2014). High-pressure Processing: Kinetic Models for Microbial and Enzyme Inactivation. Food Engineering Reviews. doi:10.1007/s12393-014-9075-x
DOI	10.1007/s12393-014-9075-x
Publisher	Springer
Version	Accepted Manuscript
Terms of Use	http://cdss.library.oregonstate.edu/sa-termsfuse

1 **High Pressure Processing: Kinetic Models for**
2 **Microbial and Enzyme Inactivation**

3 Author: Vinicio Serment-Moreno

4 *Affiliation: Centro de Biotecnología FEMSA, Escuela de Biotecnología y*
5 *Alimentos, Tecnológico de Monterrey, Av. Eugenio Garza Sada 2501 Sur, Col.*
6 *Tecnológico, 64849, Monterrey, NL, México*

7 vsermentm@gmail.com

8

9 Author: Gustavo Barbosa-Cánovas

10 *Affiliation: Center for Nonthermal Processing of Food, Washington State*
11 *University, Pullman, WA 99164-6120, U. S. A.*

12 Phone: 1-509-335-6188

13 Fax: 1-509-335-2722

14 barbosa@wsu.edu

15 www.bsyse.wsu.edu/barbosa

16

17 Corresponding Author: José Antonio Torres

18 *Affiliation: Food Process Engineering Group, Department of Food Science and*
19 *Technology, Oregon State University, 100 Wiegand Hall, Corvallis, OR 97331, U.*
20 *S. A.*

21 Phone: 1-541-737-4757

22 Fax: 1-541-737-1877

23 J_Antonio.Torres@OregonState.edu

24

25 Corresponding Author: Jorge Welti-Chanes

26 *Affiliation: Centro de Biotecnología FEMSA, Escuela de Biotecnología y*
27 *Alimentos, Tecnológico de Monterrey, Av. Eugenio Garza Sada 2501 Sur, Col.*
28 *Tecnológico, 64849, Monterrey, NL, México*

29 Phone: +52-81-8358-2000 ext. 4923

30 Fax: +52-81-8358-4923

31 jwelti@itesm.com

32

33

34 **Abstract:** High pressure processing (HPP) has become the most widely accepted
35 nonthermal food preservation technology. The pressure range for commercial
36 processes is typically around 100-600 MPa, whereas moderate temperature (up to
37 65°C) may be used to increase microbial and enzymatic inactivation levels.
38 However, these industrial processing conditions are insufficient to achieve
39 sterilization since much higher pressure levels (>1000 MPa) would be required to
40 inactivate bacterial endospores and enzymes of importance in food preservation.
41 The next generation of commercial pressure processing units will operate at about
42 90-120°C and 600-800 MPa for treatments defined as Pressure Assisted Thermal
43 Processing (PATP), or Pressure Assisted Thermal Sterilization (PATS) if the
44 commercial food sterilization level required is achieved. Most published HPP
45 kinetic studies have focused only on pressure effects on the microbial load and
46 enzyme activity in foods and model systems. Published work on primary and
47 secondary models to predict simultaneously the effect of pressure and temperature
48 on microbial and enzymatic inactivation kinetics is still incomplete. Moreover,
49 few references provide a detailed and complete analysis of theoretical, empirical,
50 and semi-empirical basis for the kinetic models proposed to predict the level of
51 microbial and enzyme inactivation achieved. This review organizes these
52 published kinetic models according to the approach used, and then presents an in-
53 depth and critical revision to define the modeling research needed to provide
54 commercial users with the computational tools needed to develop and optimize
55 pasteurization and sterilization pressure treatments.

56 *KEYWORDS: High Pressure Processing, Pressure Assisted Thermal Processing,*
57 *Primary and Secondary Models, Kinetics, Enzyme Inactivation, Microbial*
58 *Inactivation*

59

60 NOMENCLATURE

A	Enzyme activity; units mg^{-1} , units ml^{-1}
A_f	Accuracy factor
a	Linear temperature dependence of the activation volume under isobaric conditions, Eyring-Arrhenius secondary model; $\text{cm}^3 \text{mol}^{-1} \text{K}^{-1}$
a_w	Water activity
A_0	Enzyme activity prior to thermal or pressure treatments; units mg^{-1} , units ml^{-1}
A_∞	Residual enzyme activity after long thermal or pressure treatments; units mg^{-1} , units ml^{-1}
b	Slope parameter, Weibull kinetic model; min^{-n}
b'	Slope parameter, Weibull kinetic model; min^{-1}
$c_i; i=1,2,..n$	Empirical kinetic model coefficients
C	Concentration, microbial population or enzyme activity
C_P	Specific heat capacity under isobaric conditions; $\text{J mol}^{-1} \text{K}^{-1}$
C_0	Initial concentration, microbial population or enzyme activity prior to thermal or pressure treatments
C_∞	Final concentration, microbial population or enzyme activity after long thermal or pressure treatments
D_T	Decimal reduction time describing the lethal thermal effect assuming first order kinetics; s, min
D_P	Decimal reduction time describing the lethal pressure effect assuming first order kinetics; s, min
D_{Pref}	Decimal reduction time describing the lethal pressure effect at a reference pressure and assuming first order kinetics; s, min
E_a	Arrhenius activation energy describing the temperature dependence of a process kinetics; $\text{J mol}^{-1} \text{K}^{-1}$
E_{aP}	Arrhenius activation energy at a reference pressure; $\text{J mol}^{-1} \text{K}^{-1}$
$F(t)$	System failure time predicted with the Weibull distribution function; s, min
f_P	Slope parameter when pressure is the independent Weibull kinetic model variable; MPa^{-n}
f_T	Slope parameter when temperature is the independent Weibull kinetic model variable; MPa^{-n}
g	Activation energy exponential pressure dependence under isothermal conditions, Eyring-Arrhenius secondary model; MPa^{-1}
G	Gibbs free energy; J mol^{-1}
ΔG	Gibbs free energy change; J mol^{-1}
ΔG_{ref}	Gibbs free energy change at reference pressure and temperature conditions; J mol^{-1}
h	Planck constant; $6.6260 \times 10^{-34} \text{ J}\cdot\text{s}$
H	Difference between the upper and lower asymptote, log-logistic kinetic model
HPP	High Pressure Processing

k	Reaction rate constant; min^{-1}
k_B	Boltzmann constant; $1.3806 \times 10^{-23} \text{ J K}^{-1}$
k_{refP}	Reaction rate constant at a reference pressure; min^{-1}
k_{refT}	Reaction rate constant at a reference temperature; min^{-1}
k^\ddagger	Activated complex reaction rate constant; min^{-1}
K	Equilibrium constant for a reaction
K^\ddagger	Pseudo-equilibrium constant for a reactant to activated complex formation
L	Lethality; cfu s^{-1} , cfu min^{-1}
m	Exponent, Weibull log-logistic secondary model
n	Exponent, Weibull kinetic model
N	Microbial population; cfu g^{-1} , cfu ml^{-1}
N_0	Microbial population prior to thermal or pressure treatments; cfu g^{-1} , cfu ml^{-1}
N_∞	Microbial population surviving long thermal or high pressure treatments; cfu g^{-1} , cfu ml^{-1}
P	Scale parameter, Weibull distribution function
P	Pressure; MPa
P_c	Critical pressure parameter, Weibull log-logistic secondary model; MPa
P_{c0}	Critical pressure parameter at a reference temperature, Weibull exponential secondary model; MPa
P_{ref}	Reference pressure; MPa
$PATP$	Pressure assisted thermal processing
$PATS$	Pressure assisted thermal sterilization
q	Shape parameter, Weibull distribution function
r	Chemical reaction rate
R	Ideal gas constant; $8.314 \text{ J mol}^{-1} \text{ K}^{-1}$, $8.30865 \text{ cm}^3 \text{ MPa mol}^{-1} \text{ K}^{-1}$
R^2	Regression coefficient
ΔS	Entropy change, thermodynamic model; $\text{J mol}^{-1} \text{ K}^{-1}$
ΔS_{ref}	Entropy change at a reference temperature, thermodynamic model; $\text{J mol}^{-1} \text{ K}^{-1}$
t	Time; s, min
T	Temperature; K
T_c	Critical temperature parameter, Weibull log-logistic secondary model; K
T_{c0}	Critical temperature parameter at a reference temperature, Weibull exponential secondary model; K
T_{ref}	Reference temperature; K
\bar{V}_P	Partial molar volume of products in a chemical reaction; $\text{cm}^3 \text{ mol}^{-1}$

\bar{V}_R	Partial molar volume of reactants in a chemical reaction; $\text{cm}^3 \text{mol}^{-1}$
\bar{V}^\ddagger	Partial molar volume of the active complex, transitional state theory; $\text{cm}^3 \text{mol}^{-1}$
\bar{V}_T^\ddagger	Partial molar volume of the active complex at a reference temperature, transitional state theory; $\text{cm}^3 \text{mol}^{-1}$
$\Delta\bar{V}_{\text{reaction}}$	Molar volume change of a chemical reaction; $\text{cm}^3 \text{mol}^{-1}$
$\Delta\tilde{V}^\ddagger$	Molar volume change to reach the active complex, transitional state theory
w_P	Exponential pressure dependence of parameter b' , Weibull secondary model; MPa^{-1}
w_T	Exponential temperature dependence of parameter b' , Weibull secondary model; K^{-1}
z_P	Pressure resistant parameter under isothermal conditions, Bigelow model; MPa
z_T	Thermal resistant parameter under isobaric conditions, Bigelow model; K

61

62 GREEK SYMBOLS

α	Thermal expansivity coefficient, thermodynamic model; $\text{cm}^3 \text{mol}^{-1} \text{K}^{-1}$; upper asymptote, log-logistic kinetic model
$\Delta\alpha$	Thermal expansivity coefficient change under non –isothermal and –isobaric conditions; $\text{cm}^3 \text{mol}^{-1} \text{K}^{-1}$
β	Compressibility factor, thermodynamic model; $\text{cm}^6 \text{J}^{-1} \text{mol}^{-1}$; lower asymptote, log-logistic kinetics model
$\Delta\beta$	Compressibility factor change under non –isothermal and –isobaric conditions, thermodynamic model; $\text{cm}^6 \text{J}^{-1} \text{mol}^{-1}$
Ψ	Log fraction parameter, Weibull biphasic kinetic model
Ω	Maximum inactivation rate, log-logistic kinetic model; cfu s^{-1} , cfu min^{-1}
τ	Log time at which the maximum inactivation rate starts, log-logistic kinetic model; min
λ	Time interval in which no high pressure processing inactivation occurs, secondary quasi chemical kinetic model; min
v^\ddagger	Frequency at which the activated complex transforms into products, energy distribution described by the Planck equation; s^{-1}

63

64 **Introduction**

65 **Food safety and high pressure processing (HPP)**

66 High pressure processing (HPP) has successfully evolved into one of the most
67 recurrent alternatives for thermal food processing. In the last 20 years, the number
68 of HPP installations in the world, and processing a wide variety of foods, grew
69 from one in 1990 to nearly 200 units with a concurrent tenfold increase in size
70 from 25-50 L to 300-500 L (Bermúdez-Aguirre and Barbosa-Cánovas, 2011;
71 Mújica-Paz et al., 2011). In addition, the operating pressure level increased from
72 about 400 MPa to about 600-800 MPa reducing pressure holding times from 15-
73 30 minutes to a few minutes. The rapidly growing number of installed units with
74 shorter processing time and larger vessel volume has dramatically increased the
75 installed pressure processing capacity. The high consumer acceptance of HPP-
76 treatments reflects, in most cases, a minimal alteration of the original nutritional
77 and sensory food characteristics while effectively inactivating pathogens, spoilage
78 microorganisms and enzymes (Welti-Chanes et al., 2002; Barbosa-Cánovas and
79 Juliano, 2008; López-Gómez et al., 2009; Cruz et al., 2011).

80

81 **Microbial Inactivation**

82 Microorganisms are affected by several simultaneous lethal effects with cellular
83 membrane damage frequently reported as a dominant factor (Mañas and Pagán,
84 2005; Patterson, 2005; Velazquez et al., 2005; Patterson and Linton, 2009). Acyl
85 chains of the phospholipid bilayer may experience crystallization, leading to bud
86 formation, membrane rupture and intracellular material leakage (Mañas and
87 Pagán, 2005; Patterson, 2005). Low-pressure treatment levels ranging from 20-
88 180 MPa result usually in sub-lethal cellular damage. Microbial inactivation of a
89 large variety of pathogenic and spoilage bacteria vegetative forms is achieved
90 above 200-400 MPa, when irreversible protein/enzyme denaturation and
91 intracellular content leakage occurs (Lado and Yousef, 2002; Mújica-Paz et al.,
92 2011). On the other hand, HPP alone cannot inactivate bacterial spores as they can
93 withstand pressures over 1000 MPa when temperature after compression is below
94 70-80°C (Mañas and Pagán, 2005; Torres and Velazquez, 2005; Patterson and
95 Linton, 2009; Mújica-Paz et al., 2011; Reineke et al., 2011).

96 **Enzyme inactivation**

97 Protein denaturation effects vary depending on the protein structure and external
98 factors such as pressure level, temperature, pH and solvent composition (Palou et
99 al., 2007; Yaldagard et al., 2008). Irreversible changes may include dissociation of
100 oligomeric proteins into their subunits, conformational changes of the
101 substrate/active site, and aggregation or gelation of proteins due to a decrease in
102 the solution volume or the association of hydrophobic molecules (Heremans,
103 1982; Palou et al., 2007; Yaldagard et al., 2008). Reversible protein modifications
104 are typically observed in the 100-300 MPa range (Welti-Chanes et al., 2006) but
105 enzyme activity may also be enhanced within this range (Palou et al., 2007;
106 Yaldagard et al., 2008; Eisenmenger and Reyes-De-Corcuera, 2009). Some
107 enzymes can display high baroresistance, and pressures over 500 MPa combined
108 with moderate temperatures are required to induce significant inactivation.
109

110 **Current status of high pressure processing**

111 Commercial HPP units operate typically within a 100-600 MPa range and
112 temperatures between 5-65°C (Balasubramaniam et al., 2008; Bermúdez-Aguirre
113 and Barbosa-Cánovas, 2011; Mújica-Paz et al., 2011). Since these mild conditions
114 are insufficient to achieve bacterial spore inactivation, units operating at higher
115 pressure (600-800 MPa) and elevated temperature (90-120°C) will be necessary
116 (Ramirez et al., 2009; Valdez-Fragoso et al., 2011). This novel procedure, known
117 as Pressure Assisted Thermal Processing (PATP) or Pressure Assisted Thermal
118 Sterilization (PATS) if bacterial spore inactivation attaining commercial food
119 sterility is achieved, is under development. However, at PATP temperature and
120 pressure conditions significant chemical changes cannot be ignored due to their
121 potential for the breaking of covalent bonds (Torres et al., 2009; Valdez-Fragoso
122 et al., 2011). Approval has been granted by the U.S. Food and Drug
123 Administration for the commercial production of low-acid foods using PATS.
124 Mashed potatoes inoculated with *Clostridium botulinum* spores were subjected to
125 a shelf-life study under the severe conditions used when testing food supplies for
126 the United States Army. No microbial growth was observed during storage and
127 the sensory quality observed was superior to those possible with a conventional
128 thermal process (NCFST, 2009).

129 Unlike other physical and chemical factors, pressure is delivered uniformly
130 throughout the vessel almost immediately after being applied (Rauh et al., 2009).
131 As a result of this compression, the food temperature increases depending on
132 factors such as food composition, pressure level, initial food and pressurizing
133 media temperature, pressurization media used, vessel loading factor, and
134 equipment design. The rise in temperature per 100 MPa due to adiabatic
135 compression heating has been reported to be $\approx 3^{\circ}\text{C}$ for water and $\approx 8\text{-}9^{\circ}\text{C}$ for fat
136 and oils, while proteins and carbohydrates show intermediate values (Patazca et
137 al., 2007; Balasubramaniam et al., 2008; Otero et al., 2010). The prediction of the
138 temperature rise remains an area of active research.

139

140 In spite of the PATP/PATS process already approved by the FDA and suggesting
141 the upcoming commercialization of this technology, extensive databases of
142 predictive models, kinetic parameters, and standardized procedures similar to
143 those developed for conventional technologies such as thermal processing are not
144 yet available. At present, most of the kinetics information on high pressure
145 processing of foods is disperse and obtained using relatively narrow ranges for the
146 experimental pressure-temperature conditions tested. Even though the scientific
147 data obtained may be sufficient for the development of a food product, it is
148 certainly limited to evaluate the inactivation kinetics models proposed. Analysis
149 of the fit to experimental data is frequently limited to comparing a few models.
150 This review shows that many food scientists are still relying on linear inactivation
151 kinetics, even though concave and sigmoidal trends are frequently observed in
152 pressure treatments. Additionally, most of the reported HPP investigations on
153 inactivation kinetics have focused on pressure effects, and often do not take into
154 account the contribution of the temperature changes due to compression of the
155 food and pressurizing fluid, and the heat exchanges involving the product and
156 pressurization media, the vessel walls, and the equipment surroundings. When
157 accurate temperature profiles of HPP are available, inactivation kinetics models
158 should be paired with transport phenomena equations predicting the pressure-
159 temperature profiles under PATP/PATS conditions when analyzing chemical
160 reactions and the inactivation of microorganisms and enzymes in foods.
161 Therefore, the following sections review chemical and biochemical models to

162 provide a concise, analytical reference for high pressure food processing kinetic
163 models with theoretical, empirical and semi-empirical backgrounds.

164 **Primary models**

165 Primary modeling consists of developing mathematical expressions based on
166 theoretical principles, empirical observations, or the combination of both, to
167 predict changes in microbial counts, enzyme activity, or chemical concentrations
168 as a function of the processing time. According to the shape of the kinetic
169 behavior predicted, primary models are classified as linear, concave or sigmoidal.

170

171 **Linear primary models**

172 ***First order kinetics model***

173 First order kinetics continues to be the most often model to describe microbial and
174 enzyme inactivation, although poor estimates can be expected since non-linear
175 trends are often observed experimentally (Peleg, 2006; Wilson et al., 2008;
176 Corradini et al., 2009; Pilavtepe-Çelik et al., 2009). It assumes that the change in
177 chemical changes, microbial population or enzyme activity is directly proportional
178 to their concentration denoted as C in Eq. 1 and described by an inactivation rate
179 constant under constant isobaric and isothermal conditions ($k [=] \text{min}^{-1}$).

$$-\frac{dC}{dt} = k \cdot C \quad (1)$$

180

181 By integrating from $t = 0$ through treatment time t and from $C(t = 0) = C_0$ through
182 $C(t) = C$ the resultant model (Eq. 2) establishes that the Napierian logarithm of
183 C/C_0 will result in a decreasing straight line that goes through the origin.

$$\ln \frac{C}{C_0} = -k \cdot t \quad (2)$$

184

185 Microbiologists frequently transform the Napierian logarithm base of Eq. 2 to
186 decimal logarithms and report the number of decimal reductions in the microbial
187 population (Eq. 3).

$$\log_{10} \frac{N}{N_0} = -\frac{k}{2.303} \cdot t \quad (3)$$

188

189 Therefore, a decimal reduction time (D_T) can be defined as the time required at a
 190 constant lethal temperature T for a tenfold reduction in the microbial load
 191 ($\log_{10} N/N_0 = \log 0.1N_0/N_0 = -1$) (Morales-Blancas and Torres, 2003a; Toledo,
 192 2007). A similar parameter (D_P) can be defined for the effect of the lethal pressure
 193 P (Parish, 1998; Basak et al., 2001). D_P can be calculated as the negative inverse
 194 of the \log_{10} linear model slope (Eq. 4).

$$\log_{10} \frac{N}{N_0} = -\frac{1}{D_P} \cdot t \quad (4)$$

195

196 The parameter D_P varies (0.01-4 min) depending on the pressure level, the
 197 microorganism, and the interaction of intrinsic food product factors with the
 198 microorganism (Table 1). For example, *Listeria monocytogenes* has a high
 199 pressure resistance in milk ($D_P = 2.43$ - 10.99 min) and a much lower in acid media
 200 such as orange juice ($D_P = 0.87$ - 2.87 min). Bacterial spores can show great
 201 pressure resistance, but may be readily inactivated ($D_P = 0.1$ - 0.6 min) with a
 202 combination of temperatures above 100°C and pressures over 400 MPa (Table 1).

203

204 INSERT TABLE 1

205

206 **Fractional conversion and multiphasic models**

207 The fractional conversion model, a variation of the first order kinetics model, is
 208 obtained by assuming that the thermal or pressure treatment leaves a residual
 209 enzyme activity or microbial load with much higher inactivation resistance. Thus,
 210 Eq. 1 is integrated from its initial conditions ($C_0 = N_0 = A_0$; at $t = 0$) to its final
 211 conditions where the remaining microbial population or enzyme activity after a
 212 prolonged treatment time is C_∞ ($t = \infty$), yielding the fraction conversion model
 213 (Eq. 5) (Van den Broeck et al., 2000; Fachin et al., 2002; Ly-Nguyen et al., 2003;
 214 Polydera et al., 2004).

$$C = C_\infty + (C_0 - C_\infty) \cdot \exp(-k \cdot t) \quad (5)$$

215

216 A similar approach was followed to develop the multiphasic model, for which
217 populations with different resistance towards the pasteurization or sterilization
218 treatment are represented by the presence of two or more isoenzymes or microbial
219 subpopulations (Chen and Wu, 1998; Fachin et al., 2002; Peleg, 2006). The
220 simplest form of the multiphasic model considers the presence of a labile fraction
221 (C_L) that is inactivated more rapidly and a stable fraction (C_S) able to withstand
222 longer treatment times. Each fraction is inactivated at a distinct rate and the
223 concentration (C) observed represents the sum of C_L and C_S at any given time. By
224 separating Eq. 1 into the labile and stable fractions, and by solving the integral,
225 this form of the multiphasic model can be described by Eq. 6.

$$C = C_L \cdot \exp(-k_L \cdot t) + C_S \exp(-k_S \cdot t) \quad (6)$$

226
227 Campanella and Peleg (2001) reported major drawbacks of biphasic models. First
228 and probably most importantly, changes in the kinetic rate constant may occur as
229 a result of alterations in the food matrix rather than caused by populations with
230 different pressure and/or temperature resistance. These authors questioned also the
231 lack of generality of the model and considered it to be too specific. Peleg (2006)
232 suggested that if enzymatic and microbial subpopulations differing in inactivation
233 resistance do exist, they should be isolated to perform independent inactivation
234 kinetics to validate the multiphasic model.

235

236 **Concave primary models**

237 ***Weibull model***

238 Many models have been developed as alternatives to linear inactivation kinetics
239 (van Boekel, 2008). Both mechanistic and empirical equations have led to an
240 adequate fit to experimental data, but often they are too specific and/or complex
241 (Mafart et al., 2002). Several authors have considered the approach of treating
242 inactivation as the distribution of the survival microbial population/enzyme
243 activity associated to diverse factors such as differences in the treatment intensity
244 or due to an heterogeneous resistance (Mafart et al., 2002; van Boekel, 2002;
245 Peleg, 2006). The Weibull distribution (Eq. 7) is used in engineering science to
246 predict the time of failure $F(t)$ of an electronic or mechanical system (van Boekel,
247 2002). Thus, the residual microbial/enzyme activity curve can be interpreted as a

248 cumulative function of the distribution that dictates the treatment time at which
249 the microorganism or enzyme will fail to resist and result in inactivation.

$$F(t) = \exp\left[-\left(\frac{t}{p}\right)^q\right] \quad (7)$$

250

251 This function, first introduced by Peleg and Cole (1998) to model microbial
252 survival curves, has been used to describe numerous inactivation kinetics because
253 it is simple (only 2 parameters), flexible and theoretically sound (Peleg, 2006;
254 Ahn et al., 2007; Buzrul et al., 2008; Corradini et al., 2009; López-Gómez et al.,
255 2009; Pilavtepe-Çelik et al., 2009; Bermúdez-Aguirre and Barbosa-Cánovas,
256 2011; Carreño et al., 2011). For inactivation kinetics studies, Eq. 7 is frequently
257 transformed to a \log_{10} base of the survival fraction $S(t)$ as in Eq. 8 (Peleg, 2006)
258 or Eq. 9 (Corradini et al., 2005):

$$\log_{10} \frac{N}{N_0} = \log_{10} S(t) = -\frac{1}{2.303} \cdot \left(\frac{t}{b}\right)^n \quad (8)$$

$$\log_{10} S(t) = -b' \cdot t^n \quad (9)$$

259

260 The parameter n determines the shape of the survival curve (Fig. 1a), where $n < 1$
261 denotes upward concavity and $n > 1$ represents a downward concavity while $n = 1$
262 would be a *unique* case corresponding to linear or first order kinetics. Concavity
263 can be used to interpret the population inactivation resistance: (a) homogenous
264 ($n = 1$); (b) tailing or increasing resistance ($n < 1$); or, (c) decreasing resistance as
265 a result of accumulated damage to the population ($n > 1$) (Peleg, 2006). Although
266 these three resistance behaviors have been observed in modeling work, no
267 microbial physiology studies have been conducted to confirm them
268 experimentally. The parameter b determines the scale of the curve as observed in
269 Fig. 1b (van Boekel, 2002), whereas the inverse of the rate coefficient b ($b' = 1 /$
270 $2.303 b^n$) determines the slope steepness of the survival trend (Corradini et al.,
271 2005). Thus Eq. 8 can be simplified and expressed as a function of b' (Eq. 9).

272

273 INSERT FIGURE 1

274

275 As shown in Eqs. 11-13, the inverse of the parameter b' to the $-n$ th power is
276 equivalent to the decimal reduction time (D) determined with the first order
277 kinetics model (Buzrul et al., 2008):

$$\log_{10} \frac{0.1N_0}{N_0} = -1 = -b' \cdot t^n \quad (11)$$

$$1 = b' \cdot t^n \quad (12)$$

$$t = \left(\frac{1}{b'} \right)^n = D \quad (13)$$

278

279 Most studies report HPP survival curves with upward concavities yielding $n < 1$
280 and $b' < 1$ values for the Weibull model parameters with the latter increasing to
281 values in the 1-3 range and a concurrent decrease in the n parameter for more
282 severe pressure and/or temperature conditions (Table 2). This shows that the
283 accumulated damage theory was fulfilled for most of the values reported in Table
284 2, since more severe HPP conditions sensitized the population and lowered the
285 shape n parameter ($n < 1$), and higher inactivation rates were observed as the
286 slope increased ($b' > 1$). Although this model has been often applied to predict
287 microbial inactivation kinetics, no reports of its application to model the
288 inactivation of enzymes, also known to display non-linear trends, were found.
289 Finally, details on the pressure and temperature effects on the Weibull model
290 parameter are discussed in the secondary model section.

291

292 INSERT TABLE 2

293

294 Peleg (2006) highlighted that nonlinear regression procedures for either $\ln S(t)$ or
295 $\log_{10} S(t)$ as a function of t can only estimate the real parameters of the Weibull
296 distribution since deviations occur with the logarithmic transformation of Eq. 7.
297 Furthermore, Mafart et al. (2002) claimed that b' and n are strongly correlated,
298 consequently a poor estimation of either one will affect the other parameter.

299

300 **Sigmoidal primary models**

301 ***Weibull biphasic model***

302 Guan et al. (2005) found that the single term Weibull model (Eq. 9) was not
303 adequate to describe complex survival curves with more than one concavity
304 change. Coroller et al. (2006) encountered this limitation when analyzing the
305 acidic inactivation of *Listeria monocytogenes* and *Salmonella enterica*. They
306 assumed that two bacterial subpopulations were present and thus the Weibull
307 model was reparametrized as a function of the labile population fraction (f) as
308 follows:

$$N(t) = N_0 \left[f \cdot 10^{-\left(\frac{t}{b_1}\right)^{n_1}} + (1-f) \cdot 10^{-\left(\frac{t}{b_2}\right)^{n_2}} \right] \quad (13)$$

309

310 Since microbial data are frequently expressed using a decimal exponential base,
311 the fraction (f) alone may not be useful. Coroller et al. (2006) transformed f to a
312 decimal logarithmic base and introduced the parameter ψ in the Weibull multi
313 population model (Eq. 14-15). An example of a survival curve for populations
314 with different subpopulation resistance predicted with the Weibull biphasic model
315 is shown in Fig. 2.

$$\psi = \log_{10} \left(\frac{f}{1-f} \right) \quad (14)$$

$$N(t) = \frac{N_0}{1+10^\psi} \left[10^{\left[\psi - \left(\frac{t}{b_1}\right)^{n_1} \right]} + 10^{-\left(\frac{t}{b_2}\right)^{n_2}} \right] \quad (15)$$

316

317 INSERT FIGURE 2

318

319 Coroller et al. (2006) simplified Eq. 15 by defining $n = n_1 = n_2$ after demonstrating
320 statistically that the shape parameters of subpopulation 1 (n_1) and subpopulation 2
321 (n_2) did not differ significantly ($p_{value} < 0.05$). The model resulting from this
322 simplification (Eq. 16) yielded a slightly more accurate fit while reducing the
323 number of parameters for the nonlinear regression.

$$N(t) = \frac{N_0}{1 + 10^{\psi}} \left[10^{\left[\psi - \left(\frac{t}{b_1} \right)^n \right]} + 10^{-\left(\frac{t}{b_2} \right)^n} \right] \quad (16)$$

324

325 **Log-Logistic model**

326 Cole et al. (1993) developed a model to predict bacterial inactivation following
 327 sigmoidal survival curves starting from the four parameter model shown in Eq.
 328 17.

$$y = \alpha + \frac{\beta}{1 + \exp(\lambda - \delta \cdot x)} \quad (17)$$

329

330 The authors attempted to confer a biological interpretation to the parameters of
 331 Eq. 17 by applying the first and second derivative criteria (Eq. 18-19) to obtain
 332 the maximum inactivation rate (Ω), and the time at which Ω occurs (τ).

333 Afterwards, Cole et al. (1993) defined the dependent variable as the microbial
 334 population logarithm ($y = \log_{10} N$) and the independent variable as the logarithm
 335 of time ($x = \log_{10} t$). Parameter ω was defined as the difference between the lower
 336 and upper asymptotes ($\omega = \beta - \alpha$), and all three biological parameters (Ω , τ , ω)
 337 where incorporated into Eq. 17 to obtain Eq. 20. Although the expression
 338 $\log_{10} (N_{t=0})$ cannot be calculated since $\log_{10} (t = 0)$ is mathematically undefined,
 339 the expression $\log_{10} (N/N_0)$ is more commonly used to describe microbial
 340 inactivation kinetics than $\log_{10} (N)$. The authors gave no justification but assumed
 341 that $t = 0.1$ min was a good approximation for $t = 0$ min to establish the
 342 “vitalistic” log-logistic model (Eq. 21).

$$y'' = \frac{d^2 y}{dx^2} = 0 = \lambda - \delta \cdot x; \quad x = \tau = \frac{\lambda}{\delta} \quad (18)$$

$$y' \left(x = \frac{\lambda}{\delta} \right) = \frac{dy}{dx} = \frac{\delta \cdot \beta}{4}; \quad \Omega = \frac{\delta \cdot \beta}{4} \quad (19)$$

$$\log_{10} N = \alpha + \frac{\omega - \alpha}{1 + \exp \left[\frac{4 \cdot \Omega}{\omega - \alpha} (\tau - \log_{10} t) \right]} \quad (20)$$

$$\log_{10} N = \frac{\omega - \alpha}{1 + \exp\left[\frac{4 \cdot \Omega}{\omega - \alpha}(\tau - \log_{10} t)\right]} - \frac{\omega - \alpha}{1 + \exp\left[\frac{4 \cdot \Omega}{\omega - \alpha}(\tau + 1)\right]} \quad (21)$$

343 Moreover, the application of the logarithm function to the independent variable (x
 344 $= \ln t$) should have been performed prior to the derivation of Eq. 17. The
 345 evaluation of the second derivative of Eq. 17 shown in Eq. 22 indicates that the
 346 solution presented by the authors as Eq. 18 is only valid when the parameter
 347 $\delta \rightarrow \infty$. The estimation of parameters τ and Ω depend of δ being sufficiently large
 348 ($\delta \rightarrow \infty$) as seen in Eq. 18-19. Unfortunately, we could not find if Cole et al.
 349 (1993) reported whether this condition ($\delta \rightarrow \infty$) is attained for either thermal or
 350 high pressure processing microbial inactivation. Users of this model should
 351 evaluate whether the parameter delta is sufficiently large ($\delta \rightarrow \infty$) to validate the
 352 biological interpretability of the log-logistic model parameters.

$$y'' = \frac{d^2 y}{d(\ln x)^2} = \ln\left(\frac{\delta - 1}{\delta + 1}\right) = \lambda - \delta \cdot x \quad (22)$$

353
 354 Chen and Hoover (2003a) were among the first investigators to use a slightly
 355 modified “vitalistic” log-logistic model to analyze microbial inactivation by HPP
 356 (Eq. 23). These authors defined the parameter H as the difference between the
 357 upper and lower asymptotes ($H = \alpha - \beta$) and $t \sim 0$ as $t = 10^{-6}$ min. As in the case of
 358 Cole et al. (1993), Chen and Hoover (2003b) gave no explanation for the use of
 359 this latter value. The model was evaluated for the inactivation of *Yersinia*
 360 *enterocolitica* in sodium potassium buffer and in UHT whole milk subjected at
 361 room temperature to pressures within the 300-500 MPa range. The experimental
 362 survival data was described using the linear, Weibull, Gompertz and log-logistic
 363 models to identify the best inactivation model. Amidst the models tested, the log-
 364 logistic equation was most consistently the best model as denoted by its regression
 365 coefficient ($R^2 = 0.946-0.982$) and accuracy factor ($A_f = 1.047-1.144$). The values
 366 reported in Table 3 for the H parameter ranged from -4.61 to -39.71, which clearly
 367 lacks a biological or physical meaning. Consequently, Chen and Hoover (2003a)
 368 decided to fix $H = -14$ which reduced also the number of parameters (Eq. 24).
 369 Although a clear reason for selecting this value was not provided, the reduced log-
 370 logistic model (Eq. 24) gave slightly better results than the three parameter model
 371 (Eq. 23) as shown in Fig. 3.

$$\log \frac{N}{N_0} = -\frac{H}{1 + \exp\left[\frac{4 \cdot \Omega \cdot (\tau - \log t)}{H}\right]} + \frac{H}{1 + \exp\left[\frac{4 \cdot \Omega \cdot (\tau + 6)}{H}\right]} \quad (23)$$

$$\log \frac{N}{N_0} = -\frac{14}{1 + \exp\left[-\frac{\sigma \cdot (\tau - \log t)}{3.5}\right]} + \frac{14}{1 + \exp\left[-\frac{\sigma \cdot (\tau + 6)}{3.5}\right]} \quad (24)$$

372

373 INSERT FIGURE 3

374

375 Additional Weibull and log-logistic HPP inactivation kinetic model comparisons
 376 have been published for diverse pathogens and food matrixes (Buzrul and Alpas,
 377 2004; Guan et al., 2005; Guan et al., 2006; Chen, 2007; Kingsley et al., 2007;
 378 Wang et al., 2009) showing equally acceptable or slightly better predictions when
 379 using Eq. 23. The greatest advantage of the log-logistic over the Weibull model is
 380 its ability to describe sigmoidal kinetic curves without further modifications
 381 (Guan et al., 2005). However, only a few values of the log-logistic model
 382 parameters have been reported for HPP (Table 3) and no secondary models to
 383 predict pressure and temperature effects on the parameters H , Ω or τ were found
 384 when preparing this review.

385

386 INSERT TABLE 3

387 **Other primary models**

388 Other primary models commonly found for the temperature effect on microbial
 389 growth and microbial/enzyme inactivation kinetics have been used to a lesser
 390 extent when analyzing combined pressure and temperature effects on foods. They
 391 include the Baranyi-Roberts equation (Baranyi and Roberts, 1994; Pérez et al.,
 392 2007; Saucedo-Reyes et al., 2009), the Gompertz model which has consistently
 393 shown poorer fit when compared to other primary models (Chen and Hoover,
 394 2003a; Guan et al., 2005; Koseki and Yamamoto, 2007; Saucedo-Reyes et al.,
 395 2009; Vega-Gálvez et al., 2012), and the enhanced quasi-chemical kinetic model
 396 (EQCKM). Even though the latter accounts for only a few publications in the high
 397 pressure kinetics area, this model was further analyzed in this review as it
 398 represented a recent and very different modeling approach.

399

400 **Enhanced Quasi-Chemical Kinetic Model (EQCKM)**

401 Unlike most microbial predictive models which take into account only the
402 population growth or inactivation rate kinetics, the quasi-chemical model can
403 describe both phenomena individually or simultaneously (Ross et al., 2005).
404 According to the quasi chemical kinetic model (QCKM), biochemical reactions
405 occurring at the microbial level can be assumed to follow a successive four-step
406 chemical kinetics mechanism representing: (1) transition of microbial cells from
407 the lag phase to the growth stage; (2) multiplication of microorganisms in the
408 growth phase on a binary exponential basis; (3) microbial death after completing
409 the cell life cycle; and (4) microbial death by the accumulation of a non-specific
410 hazardous metabolite.

411

412 A set of chemical reaction equations relating rate constants (k) with the microbial
413 population or the hazardous metabolite concentration can be developed for each
414 step and solved as a system of ordinary differential equations (Ross et al., 2005;
415 Doona et al., 2008). The QCKM was originally developed for predictions of
416 pathogen growth under various environmental conditions differing in pH, a_w and
417 concentration of an added microbial inhibitor (Ross et al., 2005). The same
418 approach has been successfully applied to model the kinetics for the pressure
419 inactivation of *E. coli* in the 207-345 MPa and 30-50°C range (Doona et al.,
420 2005). The quasi chemical model effectively fit sigmoidal curves for *E. coli* at 40-
421 50°C, and shoulder formation but only under the mildest experimental conditions
422 (Doona et al., 2005; Doona et al., 2008). Furthermore, Doona et al. (2012)
423 reported that the QCKM failed to describe well the high pressure kinetics for the
424 inactivation of *Listeria monocytogenes* which presented “tailing”. Therefore, the
425 authors adapted the differential equations of the QCKM under a new set of
426 theoretical assumptions for the complete cell cycle under high pressure and
427 renamed it as the “enhanced” quasi-chemical kinetic model (EQCKM).

428

429 A sub-version of the EQCKM considering only microbial inactivation under high
430 pressure is shown in Figure 4. Under the assumptions of this EQCKM sub-
431 version, the population of microbial cells in the lag phase (M) subjected to
432 pressure can either become metabolically active to propagate a population in the
433 growth phase (M^*) at a very slow rate (Eq. 25), or remain in the lag phase while

434 displaying superior baroresistance (*BR*; Eq. 26). Finally, both M^* and *BR* undergo
 435 inactivation at different rates (*MD*, Eq. 27-28). First order kinetics was assumed to
 436 describe the change with time of all microbial populations assumed in this
 437 modified model (M, M^*, BR, D). Thus, each step of the EQCM (Fig. 4)
 438 corresponds to a biochemical reaction with a kinetic rate constant (k_1-k_4). Due to
 439 the presence of successive biochemical reactions, all differential equations must
 440 be solved simultaneously as shown in the analytical solution (Eq. 29a-c).
 441 However, the “true” microbial count values for M, M^* , and *BR* cannot not be
 442 determined experimentally. The experimental quantification of *L. monocytogenes*
 443 after each HPP treatment can describe only the total of the individual populations
 444 assumed in the model ($U=M+M^*+BR$; Eq. 29d) and not their individual values.
 445 The EQKM solution is found by minimizing the error between the experimental
 446 microbial plate counts (U) and sum of the predicted values.

$$M \rightarrow M^*, k_1 \quad (25) \quad \frac{dM}{dt} = -(k_1 + k_2) \cdot M \quad (29a)$$

$$M \rightarrow BR, k_2 \quad (26) \quad \frac{dM^*}{dt} = k_1 \cdot M - k_3 \cdot M^* \quad (29b)$$

$$M^* \rightarrow MD, k_3 \quad (27) \quad \frac{dBR}{dt} = k_2 \cdot M - k_4 \cdot BR \quad (29c)$$

$$BR \rightarrow MD, k_4 \quad (28) \quad U = M + M^* + BR \quad (29d)$$

447

448 INSERT FIGURE 4

449

450 Since the EQCKM describes two different inactivation rates, Doona et al. (2012)
 451 opted to validate the model by calculating the processing time (tp) required to
 452 deliver 6 log reductions of *L. monocytogenes* counts (U) for several pressure (207-
 453 414 MPa) and temperature (20-50°C) combinations. The model successfully
 454 predicted tp as shown by the low standard error values (0.09-0.46) in the pressure-
 455 temperature range studied. For all pressure/temperature combinations, the kinetic
 456 constants k_1 and k_3 were greater than k_2 and k_4 . The differences became more
 457 evident at 414 MPa, indicating that the microbial inactivation is primarily driven
 458 by pressure in the 20-50°C temperature range. Additionally, the high pressure
 459 resistance of *L. monocytogenes* was confirmed since k_3 was only significantly
 460 higher than k_4 for pressure levels over 345 MPa, and just three of the tested PATP

461 treatments yielded $tp \leq 15$ min. A key disadvantage of the EQCKM is that the key
462 variables involved (M , M^* and BR) and their relationship to experimental
463 microbial plate counts (U ; Eq. 29d) remain a theoretical construct that will be
464 difficult to confirm experimentally.

465
466

467 **Secondary Models**

468 The previously reviewed primary models are useful when the processing
469 conditions (pressure, temperature, pH, etc.) are kept constant. If any processing
470 condition is changed, a new set of experiments must be performed to obtain new
471 primary model parameters. To extend the application of primary models,
472 mathematical expressions known as secondary models can be developed to
473 estimate the pressure and/or temperature effect on the predicted primary model
474 parameters. As in the case of primary models, secondary models can be obtained
475 from theoretical considerations or empirical observations. Most of the secondary
476 models here presented are non-linear, reflecting complex biological behaviors
477 under high pressure/high temperature conditions.

478

479 **Simultaneous pressure and temperature effects on first order** 480 **kinetics parameters**

481 ***Bigelow model***

482 The Bigelow model was developed to obtain log-linear estimates of the decimal
483 reduction time as a function of temperature (Bigelow, 1921; Morales-Blancas and
484 Torres, 2003a, b). The equation became so important and broadly accepted, that
485 even nowadays it remains the standard approach in thermal processing design
486 (van Asselt and Zwietering, 2006; Holdsworth and Simpson, 2007; Daek and
487 Farkas, 2012).

488 The Bigelow model has been adopted to model the reaction rate dependence on
489 the applied pressure ($k(P)$) using z_P , defined as the inverse negative slope of log
490 D_P vs. pressure level (Eq. 30). The parameter z_P determines the pressure increase

491 required to achieve a 10-fold increase in the inactivation rate, a constant
 492 analogous to the thermal resistance constant z_T (Parish, 1998; Lado and Yousef,
 493 2002; Cook, 2003; Dogan and Erkmén, 2004; Van Opstal et al., 2005; Koo et al.,
 494 2006; Peleg, 2006; Ramos and Smith, 2009; Zhou et al., 2009).

$$z_p = -\frac{P - P_{ref}}{\log D_p - \log D_{P_{ref}}} \quad (30)$$

495
 496 Santillana Farakos and Zwietering (2011) attempted to establish a global kinetic
 497 model based on the pressure and temperature dependence of the microbial
 498 inactivation kinetics by HPP. Reported D values for first order kinetics (Table 4)
 499 were fitted to Eq. 30-32 and analyzed statistically. Both models for D (Eqs. 31-32)
 500 assume that the exponential relation of z_p and z_T was directly proportional to
 501 pressure and temperature; however, Eq. 32 includes a term describing a first order
 502 interaction between pressure and temperature. The parameter z_{PT} represents the
 503 amount that the linear term $P \cdot T$ needs to increase for a tenfold decrease in D .

$$\log D = \frac{1}{z_p} \cdot (P_{ref} - P) + \frac{1}{z_T} \cdot (T_{ref} - T) + \log D_{Pr_{ef}T_{ref}} \quad (31)$$

$$\log D = \frac{1}{z_p} \cdot (P_{ref} - P) + \frac{1}{z_T} \cdot (T_{ref} - T) + \frac{1}{z_{PT}} \cdot [(T_{ref} \cdot P_{ref}) - (T \cdot P)] + \log D_{Pr_{ef}T_{ref}} \quad (32)$$

504
 505 Santillana Farakos and Zwietering (2011) showed for Eq. 30 the lowest adjusted
 506 regression coefficient ($R^2_{adj} = -0.037-0.630$) reflecting the large influence of
 507 temperature on HPP treatments. Both models describing the pressure-temperature
 508 effect (Eqs. 31-32) had similar prediction accuracy ($R^2_{adj} = 0.30-0.87$), indicating
 509 that the linear pressure-temperature interaction has no overall significance ($p_{value} >$
 510 0.05). Thus, Santillana Farakos and Zwietering (2011) reported only the
 511 parameters for Eq. 31 (Table 4). Bacterial spores displayed the highest pressure
 512 resistance constant ($z_p = 614-616$ MPa), followed by vegetative cells ($z_p = 206-$
 513 385 MPa), and yeasts ($z_p = 91$ MPa). Conversely, under high pressure the
 514 temperature effect on yeast inactivation was less significant ($z_T = 141$ °C) than the
 515 observed for vegetative cells ($z_T = 38-97$ °C) and spores ($z_T = 20-45$ °C), since
 516 yeasts are readily inactivated by pressure alone. The *Vibrio* species (spp.) was the
 517 only microorganism to be more readily inactivated when temperature was lowered

518 ($z_T = -18.4 \pm 2.3$). The authors highlighted the need to avoid using these models for
 519 nonlinear inactivation curves, since under- or overestimation may occur
 520 (Santillana Farakos and Zwietering, 2011).

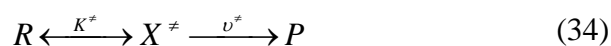
521 INSERT TABLE 4

522 **Pressure kinetics fundamentals**

523 The Le Chatelier principle states that *under equilibrium*, a system subjected to
 524 pressure will adopt the molecular configurations, chemical interactions, and
 525 chemical reactions yielding the smallest overall volume (Farkas and Hoover,
 526 2000; Welte-Chanes et al., 2006; Balasubramaniam et al., 2008). Mathematically,
 527 the Le Chatelier principle has been expressed with thermodynamic relations by
 528 using the partial molar volume (\bar{V}) concept originally defined for gas mixtures.
 529 The overall molar volume change for the reaction ($\overline{\Delta V_{reaction}}$) defined as the
 530 difference in the partial molar volumes of products and reactants (Eq. 33) can be
 531 expressed as the change of the Gibbs energy with respect to pressure at a constant
 532 temperature. Thus, $\overline{\Delta V_{reaction}}$ is related directly to the equilibrium constant (K) for
 533 the reaction (Smith et al., 1997).

$$\overline{\Delta V_{reaction}} = \sum \bar{V}_P - \sum \bar{V}_R = \left(\frac{\partial \Delta G}{\partial P} \right)_T = -RT \left(\frac{\partial \ln K}{\partial P} \right)_T \quad (33)$$

534
 535 This description is further extrapolated to biological systems under the
 536 *Transitional State Theory* by proposing the existence of a biological reactant (R)
 537 in equilibrium with an activated biological complex (X^\ddagger) prior to the formation of
 538 the biological reaction product P (Eq. 34). If the formation of the activated
 539 complex is in thermal equilibrium, the frequency (ν^\ddagger) at which X^\ddagger transforms into
 540 P can be calculated using quantum ($E = h \cdot \nu^\ddagger$) and classical physics ($E = k_B \cdot T/h$)
 541 equations describing the internal energy distribution (Eq. 35):



$$\nu^\ddagger = \frac{k_B \cdot T}{h} \quad (35)$$

542

543 where h is the Planck constant ($6.626 \times 10^{-34} \text{ J s}^{-1}$), k_B is the Boltzmann constant
 544 ($1.38 \times 10^{-23} \text{ J K}^{-1}$), and T (K) is the absolute temperature at which the chemical
 545 reaction takes place (Missen et al., 1999; Leskovac, 2003). Hence, the product
 546 formation rate equation (r_p ; Eq. 36) can be rewritten to yield Eq. 38 by
 547 substituting v^\ddagger (Eq. 35) and the pseudo-equilibrium constant K^\ddagger (Eq. 37) to obtain
 548 a theoretical definition of the kinetic rate constant k (Eq. 39).

$$r_p = v^\ddagger \cdot [X^\ddagger] \quad (36)$$

$$K^\ddagger = \frac{[X^\ddagger]}{[R]} \quad (37)$$

$$r_p = \frac{k_B \cdot T}{h} \cdot K^\ddagger \cdot [R] \quad (38)$$

$$k = \frac{k_B \cdot T}{h} \cdot K^\ddagger \quad (39)$$

549
 550 To depict the effect of pressure on the kinetic rate constant for isothermal
 551 conditions, Eq. 39 can be used to substitute K^\ddagger in Eq. 33. The Gibbs free energy
 552 and volume change are state functions and a reference pressure (P_{ref}) must be
 553 selected arbitrarily when quantifying these thermodynamic properties. By
 554 integrating of Eq. 40 from P_{ref} to P , and defining the kinetic constant with respect
 555 to the reference conditions (k_{ref}) yields the Eyring model (Eq. 42), where the term
 556 $h/k_B \cdot T$ is a constant and its derivative equals zero (Eq. 41).

$$\left[\frac{\partial \ln K^\ddagger}{\partial P} \right]_T = \frac{\partial}{\partial P} \left[\ln \left(\frac{k \cdot h}{k_B \cdot T} \right) \right]_T \quad (40)$$

$$\frac{\partial}{\partial P} \left[\ln k + \ln \left(\frac{h}{k_B \cdot T} \right) \right]_T = \left[\frac{\partial (\ln k)}{\partial P} \right]_T = - \frac{\Delta V^\ddagger}{R \cdot T} \quad (41)$$

$$\ln k = \ln k_{ref} - \frac{\Delta V^\ddagger \cdot (P - P_{ref})}{R \cdot T} \quad (42)$$

557
 558 According to the Eyring equation (Eq. 42), the slope of the plot $\ln k$ vs. P under
 559 isothermal conditions is an estimation of the volume change between the activated
 560 complex and the reactants (ΔV^\ddagger), also known as the *activation volume*. Thus, the
 561 formation of the active complex and/or products are accelerated when the overall
 562 reaction volume is decreased ($\Delta V^\ddagger < 0$) (Heremans, 1982). Conversely, $\Delta V^\ddagger > 0$

563 suggests that pressure will inhibit the active complex formation and/or its
 564 subsequent transformation into products, whereas $\Delta V^\ddagger = 0$ indicates that the
 565 reaction rate is not affected by pressure. The pressure dependence of ΔV^\ddagger
 566 commonly deviates from the linear behavior dictated by the Eyring model (Eq.
 567 42) and either theoretical or empirical approximations must be followed, as
 568 discussed in the following sections (Isaacs, 1981; Weemaes et al., 1998a; Van den
 569 Broeck et al., 2000; House, 2007; Segovia Bravo et al., 2012).

570

571 It is also important to stress that the *Transition State Theory* is an extension of the
 572 collision rate theory of gas phase kinetics. Although, the *Transition State Theory*
 573 is apparently valid to describe both gas and liquid phase kinetics in practice, a
 574 rigorous theoretical approach to liquid phase kinetics involves the determination
 575 of other critical features such as electrochemical and transport phenomena
 576 properties of all components in the solution (Atkins and de Paula, 2006), which
 577 would be very challenging, and probably impossible to determine in complex
 578 matrixes such as foods.

579 ***Eyring-Arrhenius model***

580 A mathematical model describing the combined effects of pressure (P) and
 581 temperature (T) on the inactivation rate constant (k) developed from the
 582 exponential form of the Eyring (Eq. 43) and Arrhenius equations (Eq. 44), has
 583 been reported by several authors (Weemaes et al., 1998b; Van den Broeck et al.,
 584 2000; Polydera et al., 2004; Katsaros et al., 2010).

$$k(P) = k_{refP} \cdot \exp\left[-\frac{\Delta V^\ddagger(T)}{R} \cdot \frac{(P - P_{ref})}{T}\right] \quad (43)$$

$$k(T) = k_{refT} \cdot \exp\left[-\frac{E_a(P)}{R} \cdot \left(\frac{1}{T} - \frac{1}{T_{ref}}\right)\right] \quad (44)$$

585

586 The value of the activation energy (E_a) and activation volume (V^\ddagger) parameters
 587 change with the vessel pressure and temperature, respectively. For example, the
 588 inactivation rate of orange juice pectinmethylesterase (PME, 100-800 MPa, 30-

589 60°C) showed a linear dependence of ΔV^\ddagger with respect to temperature (Eq. 45),
 590 whereas E_a and pressure were related exponentially (Eq. 46) (Polydera et al.,
 591 2004).

$$\Delta V^\ddagger(T) = a \cdot (T - T_{ref}) + \Delta V_T^\ddagger \quad (45)$$

$$E_a(P) = E_{aP} \cdot \exp[-g \cdot (P - P_{ref})] \quad (46)$$

592

593 The double integration of the inactivation rate constant (k) with respect to pressure
 594 and temperature yields Eq. 47:

$$k = k_{refP,T} \cdot \exp\left\{-\frac{E_{aP}}{R} \cdot \exp[-g \cdot (P - P_{ref})] \cdot \left(\frac{1}{T} - \frac{1}{T_{ref}}\right) - \frac{a \cdot (T - T_{ref}) + \Delta V_T^\ddagger}{R} \cdot \frac{P - P_{ref}}{T}\right\} \quad (47)$$

595

596 This particular model deviated at low pressure (100-250 MPa) and moderate
 597 temperature ranging from 30-40°C (Polydera et al., 2004), and therefore these
 598 conditions were not taken into account for $k(P,T)$ predictions (Figure 5a).
 599 However, Katsaros et al. (2010) obtained a good correlation ($R^2 = 0.993$) between
 600 experimental and predicted values of orange PME inactivation within 100-500
 601 MPa and 20-40°C when applying the same model (Fig. 5b). The different
 602 outcomes obtained by Polydera et al. (2004) and Katsaros et al. (2010) may reflect
 603 differences in the orange variety and experimental conditions used. Although the
 604 Eyring-Arrhenius modeling of the experimental data was performed using the
 605 same software, differences were observed in the estimated activation energy
 606 (Table 5), i.e., $E_a = 148 \text{ KJ mol}^{-1}$ (Polydera et al., 2004) and $E_a = 95 \text{ KJ mol}^{-1}$
 607 (Katsaros et al., 2010). It should be noted that the latter authors used narrower
 608 pressure and temperature ranges, and the reference conditions (P_{ref}, T_{ref}) for Eq. 47
 609 were not the same. Katsaros et al. (2010) chose 300 MPa and 308 K whereas
 610 Polydera et al. (2004) selected reference conditions close to the region with the
 611 most significant enzymatic inactivation observed (600 MPa, 50°C). The Eyring-
 612 Arrhenius parameters obtained by Polydera et al. (2004) failed to consistently
 613 estimate $k(P,T)$ in the entire experimental range. Predictions of the kinetic rate
 614 constant were inaccurate at 100-250 MPa, but the model fit significantly improved
 615 in the proximity of the reference conditions selected (400-800 MPa, 40-60°C).

616

617 INSERT FIGURE 5

618

619 Weemaes et al. (1998b) and van den Broeck et al. (2000) encountered antagonistic
620 pressure effects on k , since the enzyme was stabilized at pressures below 250-350
621 MPa for orange juice PME (Figure 6) and also for avocado polyphenoloxidase
622 (PPO). The Eyring relation (Eq. 43) was not constant throughout the tested
623 pressure range and both Weemaes et al. (1998b) and van den Broeck et al. (2000)
624 opted to apply an empirical model to estimate pressure dependence of k_{ref} (Eq.
625 48). Weemaes et al. (1998b) found that the activation energy decayed
626 exponentially as the pressure system increased (Eq. 49), whereas van den Broeck
627 et al. (2000) reported a linear function for $E_a(P)$ (Eq. 50).

$$\ln k_{ref}(P) = c_1 + c_2 \cdot P + c_3 \cdot P^2 + c_4 \cdot P^3 \quad (48)$$

$$E_a(P) = E_{aP} \cdot [\exp(-c_5 \cdot P)] \quad (49)$$

$$E_a(P) = c_5 - c_6 \cdot P \quad (50)$$

628

629 INSERT FIGURE 6

630

631 The substitution of $E_a(P)$ and $k_{ref}(P)$ in the Arrhenius equation (Eq. 44) yields
632 two empirical models describing the effects of pressure and temperature on k (Eq.
633 51-52). Empirical parameters c_1 - c_4 describe the effect of pressure on k_{ref} and the
634 calculated values for PPO (Weemaes et al., 1998b) and PME (Van den Broeck et
635 al., 2000) are very similar (Table 5).

$$k = \exp \left\{ c_1 + c_2 \cdot P + c_3 \cdot P^2 + c_4 \cdot P^3 + \left[-\frac{E_{aP} \cdot [\exp(-c_5 \cdot P)]}{R} \left(\frac{1}{T} - \frac{1}{T_{ref}} \right) \right] \right\} \quad (51)$$

$$k = \exp \left\{ c_1 + c_2 \cdot P + c_3 \cdot P^2 + c_4 \cdot P^3 + \left[-\frac{c_5 - c_6 \cdot P}{R} \left(\frac{1}{T} - \frac{1}{T_{ref}} \right) \right] \right\} \quad (52)$$

636

637 Conversely, Ludikhuyze et al. (1998b, a) found that elevating pressure increased
638 the inactivation rates at all temperatures and therefore the Eyring model (Eq. 43)
639 was valid for lipoxygenase (LOX) inactivation at 50-800 MPa and 10-64°C.
640 Antagonistic effects for combined pressure-temperature treatments were again
641 present for the low temperature ($T < 40^\circ\text{C}$) and high pressure ($P > 475$ MPa)
642 region and minimum values were registered between 30-40°C. In this case, the

643 Arrhenius model (Eq. 44) could not be applied as denoted by the calculated E_a
 644 values, which were negative for $T < 40^\circ\text{C}$ and positive for $T > 40^\circ\text{C}$. Therefore
 645 Ludikhuyze et al. (1998a) elaborated an empirical model for $k_{ref}(T)$ (Eq. 53) and
 646 $\Delta V^\ddagger(T)$ (Eq. 54). The incorporation of Eq. 53-54 into the Eyring equation resulted
 647 in an Eyring-empirical secondary model (Eq. 55).

$$\ln k_{ref}(T) = c_1 + c_2 \cdot T + c_3 \cdot T^2 \quad (53)$$

$$\Delta V^\ddagger(T) = c_4 \cdot T \cdot [\exp(-c_5 \cdot T)] \quad (54)$$

$$\ln k = c_1 + c_2 \cdot T + c_3 \cdot T^2 - \left\{ \frac{c_4 \cdot T \cdot [\exp(-c_5 \cdot T)]}{R \cdot T} \cdot (P - P_{ref}) \right\} \quad (55)$$

648
 649 Doona et al. (2012) predicted the processing time ($tp = 1/k$) required to achieve 6
 650 log reductions of *L. monocytogenes* as a function of pressure and temperature with
 651 empirical models based on the Eyring and the Arrhenius equations. The pressure
 652 dependence of $\ln k$ was not linear and the authors decided to include the effect of
 653 pressure on ΔV^\ddagger , given by the compressibility factor $\Delta\beta$ and defined through Eq.
 654 56-58-56 (Morild, 1981; Van Eldik et al., 1989; Doona et al., 2012).

$$\Delta\beta = \left(\frac{\partial \Delta V^\ddagger}{\partial P} \right)_T = -R \cdot T \cdot \left(\frac{\partial^2 \ln k}{\partial P^2} \right)_T \quad (56)$$

$$\left(\frac{\partial \ln k}{\partial P} \right)_T = -\frac{1}{R \cdot T} \cdot [\Delta\beta \cdot (P - P_{ref}) + \Delta V^\ddagger] \quad (57)$$

$$\ln k = \ln k_{ref} - \frac{\Delta V^\ddagger \cdot (P - P_{ref})}{R \cdot T} + \frac{\Delta\beta \cdot (P - P_{ref})^2}{2 \cdot R \cdot T} \quad (58)$$

655
 656 Furthermore, the extended Eyring model (Eq. 56) was reparametrized by defining
 657 tp , γ as in Eq. (59, 60), $P_{ref} = 6.98 \text{ MPa}$ ($\approx 1 \text{ kpsi}$), and regrouping all terms (Eq.
 658 61-64) to yield a linear quadratic equation with three parameters (Eq. 63). Similar
 659 modifications were performed for the Arrhenius equation (model not shown), and
 660 the temperature dependence of tp was modeled with a non-dimensional linear first
 661 order equation. Doona et al. (2012) reported that both of the secondary models
 662 accurately predicted tp for a new set of experimental under isothermal or isobaric
 663 conditions.

$$\gamma = \frac{1}{P_{ref}} \cdot (P - P_{ref}) = \frac{P}{P_{ref}} = 1 + \gamma \quad (59)$$

$$tp = \frac{1}{k} \quad (60)$$

$$k = A \cdot \exp(-c_1 \cdot \gamma) \cdot \exp(-c_2 \cdot \gamma^2) \quad (61)$$

$$A = k_{ref} \cdot \exp\left[-\left(\frac{\Delta V^\ddagger \cdot P_{ref}}{R \cdot T} - \frac{\Delta\beta \cdot P_{ref}^2}{2 \cdot R \cdot T}\right)\right]; c_0 = \ln \frac{1}{A} \quad (62)$$

$$c_1 = \frac{\Delta V^\ddagger \cdot P_{ref}}{R \cdot T} - \frac{\Delta\beta \cdot P_{ref}^2}{R \cdot T} \quad (63)$$

$$c_2 = -\frac{\Delta\beta \cdot P_{ref}^2}{2 \cdot R \cdot T} \quad (64)$$

$$\ln tp = c_0 + c_1 \cdot \gamma - c_2 \cdot \gamma^2 \quad (65)$$

664

665 For microbial inactivation Katsaros et al. (2010) modified Eq. 43-44 by defining
 666 $k(T)$ and $k(P)$ as a function of decimal reduction times of *Lactobacillus brevis*
 667 and *Lactobacillus plantarum* in orange juice at reference conditions (D_{Tref} , D_{Pref})
 668 and parameters z_T and z_P as in Eq. 66-67.

$$k(T) = \frac{2.303}{D_{Tref} \cdot 10^{\left(\frac{T-T_{ref}}{z}\right)}} \quad (66)$$

$$k(P) = \frac{2.303}{D_{Pref} \cdot 10^{\left(\frac{P-P_{ref}}{z}\right)}} \quad (67)$$

669

670 Both $k(T)$ and $k(P)$ were associated by assuming an Arrhenius type relationship
 671 and an expression relating decimal reduction time (D) with the processing
 672 conditions P and T (Eq. 68).

$$D = D_{ref} \cdot \left(\exp \left\{ \begin{array}{l} -\frac{2.303 \cdot T \cdot T_{ref}}{z_T} \cdot \exp[-g \cdot (P - P_{ref})] \cdot \left(\frac{1}{T} - \frac{1}{T_{ref}} \right) \\ + \frac{2.303 \cdot (P - P_{ref})}{z_P \cdot R} \end{array} \right\} \right)^{-1} \quad (68)$$

673

674 Katsaros et al. (2010) reported a good fit for predicted $k(P, T)$ of *L. brevis* and *L.*
 675 *plantarum* in orange juice ($R^2 = 0.951$ and 0.977 , respectively) inactivation in the
 676 100-500 MPa and 20-40°C range. Pressure resistance at the reference temperature

677 was almost the same for *L. brevis* ($z_P = 94.7 \pm 7.8$ MPa) and *L. plantarum* ($z_P =$
678 95.0 ± 11 MPa). Nonetheless, thermal sensibility was lower for the former ($z_T =$
679 23.8 ± 2.4 °C) than for the latter ($z_T = 23.8 \pm 2.4$ °C and the decimal reduction time at
680 reference conditions was 2.1 min higher (Table 5).

681

682 Although decimal reduction times for the inactivation of enzymes are rarely
683 reported, Ludikhuyze et al. (2000) attempted to fit the Bigelow model (Eq. 28) to
684 the inactivation of raw bovine milk alkaline phosphatase (0.1-700 MPa; 25-63°C).
685 Enzyme activity kinetics followed a first order kinetics, and therefore k was
686 related to decimal reduction times as in Eq. (66-67). Adverse effects of PATP
687 were once again present for the low pressure/high temperature region, and the
688 pressure dependent terms (Eq. 67) were not valid in the experimental range tested.
689 Ludikhuyze et al. (2000) opted to fit experimental $D(T,P)$ values to the empirical
690 model shown in Eq. 69 (Table 5), and reported that 95% of the predicted data
691 points showed less than 15% of error when compared to the experimental values.
692 Parameter c_1 could represent D_T at a reference temperature, and the calculated
693 value at $T_{ref} = 50$ °C was $D_T = 3.33$ min (Table 5), implying that alkaline
694 phosphatase has an elevated thermal resistance.

$$\log_{10} D(P,T) = c_1 + c_2 \cdot P + c_3 \cdot P^2 - \frac{T - T_{ref}}{c_4 + c_5 \cdot P + c_6 \cdot P^2} \quad (69)$$

695

696 Hashizume et al. (1995) studied the effect of high pressure (120-300 MPa) and
697 sub-zero temperatures (-20 to 50°C) on *S. cerevisiae* inactivation. Inactivation
698 kinetics apparently followed first order kinetics at all temperatures, whereas
699 pressures below 180 MPa and temperatures between 0-40°C caused only a minor
700 microbial inactivation. A quadratic model (Eq. 70) was utilized to predict k as a
701 function of both pressure and temperature. The isokinetic rate diagrams for *S.*
702 *cerevisiae* inactivation presented an elliptical trend similar to a protein
703 denaturation diagram (Heremans and Smeller, 1998; Velazquez et al., 2005;
704 Meersman et al., 2006). Hashizume et al. (1995) concluded that the resemblance
705 of microbial and enzymatic isorate contours may be due to the adverse effects of
706 HPP on key enzymatic processes of microorganisms. Furthermore, Reynolds et al.
707 (2000) demonstrated statistically a slightly improved prediction of decimal
708 reduction times for *Z. bailii* when the linear pressure-temperature term, denoted

709 by $(P - P_{ref}) \cdot (T - T_{ref})$ was omitted (Eq. 71). The values for the parameters of Eq.
 710 70-71 are shown in Table 5.

$$\log_{10} k(P, T) = c_1 + c_2 \cdot (P - P_{ref}) + c_3 \cdot (T - T_{ref}) + c_4 \cdot (P - P_{ref})^2 + c_5 \cdot (P - P_{ref}) \cdot (T - T_{ref}) + c_6 \cdot (T - T_{ref})^2 \quad (70)$$

$$\log_{10} D(P, T) = c_1 + c_2 \cdot (P - P_{ref}) + c_3 \cdot (T - T_{ref}) + c_4 \cdot (P - P_{ref})^2 + c_5 \cdot (T - T_{ref})^2 \quad (71)$$

711

712 INSERT TABLE 5

713

714 Even though there are other empirical pressure-temperature secondary models,
 715 care must be taken when using them since most lack generality and have validity
 716 only for the specific inactivation study for which the equation was developed.
 717 Additionally, most of these polynomial parameters also lack a comprehensible
 718 biological or physical basis, and may include severe and numerous slope changes
 719 over a wide range leading to incorrect estimations of kinetics parameters.

720 ***Thermodynamic model***

721 Hawley (1971) developed a purely thermodynamic model to describe ΔG for the
 722 reversible pressure-temperature denaturation of chymotrypsinogen at 0.1-700
 723 MPa and 8.5-70°C. By integrating the general free Gibbs energy equation (Eq.
 724 72), and including the compressibility factor (β), thermal expansivity (α) and
 725 specific heat (C_p) contribution with the Maxwell relations, the result is the model
 726 proposed by Hawley (1971) shown below (Eq. 73):

$$d(\Delta G) = -\Delta S dT + \Delta V dP \quad (72)$$

$$\Delta G = \frac{\Delta\beta}{2 \cdot R \cdot T} \cdot (P - P_{ref})^2 + \frac{\Delta\alpha}{R \cdot T} \cdot (P - P_{ref}) \cdot (T - T_{ref}) - \frac{\Delta C_p}{R \cdot T} \left[T \left(\ln \frac{T}{T_{ref}} - 1 \right) + T_{ref} \right] + \frac{\Delta V_{ref}}{R \cdot T} \cdot (P - P_{ref}) - \frac{\Delta S_{ref}}{R \cdot T} \cdot (T - T_{ref}) + \Delta G_{ref} \quad (73)$$

727

728 Eq. 73 could be incorporated into the model that relates the equilibrium constant
 729 (K^\ddagger) between the reactants and the activated complex with the chemical reaction
 730 constant k described by the Transitional State Theory (See the *Pressure*
 731 *Thermodynamics Fundamentals* section) and the general ΔG equilibrium model
 732 (Eq. 72). The combination of Eq. 72-74- yields the thermodynamic kinetic model

733 (Eq. 75) (Morild, 1981; Weemaes et al., 1998b; Fachin et al., 2002; Ludikhuyze et
 734 al., 2002):

$$\Delta G = -R \cdot T \cdot \ln K \quad (74)$$

$$\begin{aligned} \ln k = & \frac{\Delta\beta}{2 \cdot R \cdot T} \cdot (P - P_{ref})^2 + \frac{\Delta V_{ref}^{\ddagger}}{R \cdot T} \cdot (P - P_{ref}) - \frac{\Delta S_{ref}}{R \cdot T} \cdot (T - T_{ref}) \\ & + \frac{\Delta\alpha}{R \cdot T} (P - P_{ref}) \cdot (T - T_{ref}) - \frac{\Delta C_p}{R \cdot T} \cdot \left\{ T \cdot \left[\ln \left(\frac{T}{T_{ref}} \right) - 1 \right] + T_{ref} \right\} + \ln k_{ref} \end{aligned} \quad (75)$$

735

736 The thermodynamic kinetic model accurately fit experimental k values for the
 737 inactivation of soybean lipoxygenase (LOX) in Tris-HCl buffer (Indrawati et al.,
 738 1999), green pea juice and intact green peas (Indrawati et al., 2001) over wide
 739 pressure-temperature ranges (Table 6). Weemaes et al. (1998b) rejected this
 740 kinetic model (Eq. 75) for the case of PME inactivation because the statistical
 741 analysis showed that the residuals for k as a function of pressure were not
 742 randomly distributed. Weemaes et al. (1998b) stated that Eq. 75 could not be
 743 applied for avocado PPO inactivation because Hawley (1971) originally
 744 developed the thermodynamic model to describe the *reversible* inactivation of
 745 chymotrypsinogen. The authors concluded that *irreversible* enzyme inactivation
 746 mechanisms differ from those for *reversible* inactivation, and therefore a different
 747 mathematical model to estimate $k(P, T)$ should be used.

748

749 In addition, the thermodynamic model proposed by Hawley (1971) assumes that
 750 thermophysical parameters ΔC_p , $\Delta\alpha$ and $\Delta\beta$ remain constant for all pressure and
 751 temperature values, which may not always be the case (Smeller, 2002). The
 752 general ΔG equation (Eq. 70) could be approximated using a Taylor expansion
 753 series (Eq. 76) where the additional third degree terms would represent the
 754 pressure and temperature dependence of ΔC_p , $\Delta\alpha$ and $\Delta\beta$ (Clark, 1979; Heremans
 755 and Smeller, 1998; Smeller, 2002; Borda et al., 2004).

$$\begin{aligned} \Delta G = & \Delta G_{ref} + \Delta V_{ref} \cdot (P - P_{ref}) - \Delta S_{ref} \cdot (T - T_{ref}) + \frac{\Delta\beta}{2} \cdot \Delta V_{ref} \cdot (P - P_{ref})^2 \\ & + \Delta\alpha \cdot (P - P_{ref}) \cdot (T - T_{ref}) - \frac{\Delta C_p}{2 \cdot T_{ref}} \cdot (T - T_{ref})^2 \end{aligned} \quad (76)$$

756

757 Ly-Nguyen et al. (2003) incorporated additional polynomial degree terms given
 758 by the Taylor expansion series (Eq. 77), and the distortion of the elliptical trend of
 759 the iso-rate contour plot reported by other authors was also observed (Smeller,
 760 2002; Borda et al., 2004).

$$\frac{\Delta\beta_2}{2 \cdot R \cdot T} \cdot (P - P_{ref})^3 + \frac{\Delta C_{p2}}{2 \cdot R \cdot T \cdot T_{ref}} \cdot (T - T_{ref})^3 + \frac{2 \cdot \Delta\alpha_2}{R \cdot T} \cdot (P - P_{ref})^2 \cdot (T - T_{ref}) \quad (77)$$

761
 762 The addition of these higher order terms yielded a better fit ($R^2 = 0.941$) than the
 763 original Hawley model ($R^2 = 0.891$) for carrot PME inactivation in the 100-825
 764 MPa and 10-65°C range (Ly-Nguyen et al., 2003). Antagonistic pressure-
 765 temperature effects were observed as the value of $\ln k$ decreased, particularly at
 766 50-65°C and 100-300 MPa (Figure 7). Apparently the inactivation rate values
 767 increased exponentially until reaching the high pressure (600-800 MPa), low
 768 temperature region (10-40°C), where an asymptotic trend was observed (Fig. 7a-
 769 7b). For moderate temperatures (50-65°C), the antagonistic effects were clearly
 770 noticeable in the 100-400 MPa region. The second order thermodynamic model
 771 (Eq. 76) failed to adjust to the lower experimental k values (Fig. 7c-7d).

772

773 INSERT FIGURE 7

774

775 Another modification of the thermodynamic model (Eq. 75) was proposed by
 776 Fachin et al. (2002) who noted that the isorate contour plots for different pressure-
 777 temperature combinations displayed no elliptical trend for the tomato PG
 778 inactivation kinetics. Consequently, the compressibility factor (β) and the specific
 779 heat capacity (C_p) from the thermodynamic model were removed (Eq. 78) because
 780 the authors stated that these terms are related to the elliptical trend. Fachin et al.
 781 (2002) found a satisfactory correlation ($R^2 = 0.92$) between experimental data and
 782 estimated $k(P, T)$ values using the reduced thermodynamic model (Eq. 76).
 783 However, the kinetic study on the inactivation of tomato PG covered a narrower
 784 pressure-temperature range (300-600 MPa, 5-50°C) as compared to the other HPP
 785 enzyme inactivation cases presented in Table 6. Therefore, the pressure and
 786 temperature range used by these authors may have affected the shape of the
 787 isorate contour plots.

$$\ln k = \frac{\Delta V_{ref}^{\ddagger}}{R \cdot T} \cdot (P - P_{ref}) - \frac{\Delta S_{ref}^{\ddagger}}{R \cdot T} \cdot (T - T_{ref}) + \frac{\Delta \alpha}{R \cdot T} \cdot (P - P_{ref}) \cdot (T - T_{ref}) + \ln k_{ref} \quad (78)$$

788

789 INSERT TABLE 6

790

791 The thermodynamic model can simultaneously describe pressure and temperature
 792 effects on the inactivation rate constants with a solid theoretical background that
 793 can be interpreted physically. Most importantly, a thermodynamic model can
 794 describe experimental data with antagonistic pressure-temperature effects while
 795 still yielding accurate predictions (Indrawati et al., 1999; Indrawati et al., 2001;
 796 Ly-Nguyen et al., 2003). However, the large number of parameters involved
 797 implies an extensive experimental plan covering a wide pressure-temperature
 798 range which makes them potentially impractical to use (Morild, 1981; Indrawati et
 799 al., 1999; Ly-Nguyen et al., 2003).

800

801 **Simultaneous pressure and temperature effects on Weibull model** 802 **parameters**

803 Peleg et al. (2002) questioned the application of the Arrhenius model to describe
 804 the temperature effect on inactivation kinetics, arguing the existence of
 805 temperature regions where the reaction system remains inert. The authors cited as
 806 an example oxidation and browning reactions, which become significant only
 807 when the temperature is increased. On the other hand, the parameters b' and n of
 808 the Weibull power law model are not necessarily constant and depend on the
 809 pressure and temperature condition applied (Peleg, 2006). Peleg et al. (2002)
 810 suggested a log-logistic model to simulate null reaction rates for low temperature
 811 regions, and a subsequent increase beyond a critical temperature level (T_c).
 812 Corradini et al. (2005) applied the log-logistic model to describe the Weibull rate
 813 parameter b' as a function of temperature (Eq. 79).

$$b'(T) = \ln\{1 + \exp[w_T(T - T_c)]\}^m \quad (79)$$

814

815 The parameter T_c denotes the temperature at which $b'(T)$ increases linearly for m
 816 $= 1$. If $T > T_c$, the parameter $b'(T)$ increases to the power $w_T(T - T_c)$, where w_T
 817 determines the rate at which $b'(T)$ increases with temperature. Conversely, when

818 $T < T_c$ the exponential term tends to zero and $b'(T)$ is approximately $\ln(1) = 0$.
 819 This model may be applied also for high pressure inactivation (Eq. 80) under
 820 isothermal conditions (Peleg, 2006; Corradini et al., 2009).

$$b'(P) = \ln\{1 + \exp[w_p(P - P_c)]\}^m \quad (80)$$

821
 822 Pressure and temperature increases are expected to lower parameters T_c and P_c
 823 (Eq. 81-82) since inactivation should be favored by more severe treatments (Peleg
 824 et al., 2005). However, these exponential-logistic models may not accurately
 825 predict antagonistic pressure-temperature effects as in the case of PME.

$$P_c(T) = P_{c0} \cdot \exp(-w_1 \cdot T) \quad (81)$$

$$T_c(P) = T_{c0} \cdot \exp(-w_2 \cdot P) \quad (82)$$

826
 827 The pressure effect on the parameter b' may be expressed also using the Bigelow
 828 model (Eq. 83) as reported by Pilavtepe-Çelik et al. (2009) or as a simple linear
 829 model as shown in Eq. 84 (Chen and Hoover, 2003a).

$$\log_{10} b' = \log_{10} b'_{ref} - \left(\frac{P - P_{ref}}{z} \right) \quad (83)$$

$$b' = slope + intercept \quad (84)$$

830
 831 The shape parameter n of the Weibull inactivation model (Eq. 9) has often been
 832 reported to display a slight or no temperature dependence (van Boekel, 2002;
 833 Buzrul et al., 2008). This statement can sometimes be assumed for $n(P)$ as Chen
 834 and Hoover (2003a) did at certain pressure ranges for *Yersinia enterocolitica*
 835 ATCC 35669 inactivation kinetics in milk and sodium phosphate buffer. No
 836 significant differences were found for n in the 300-400 MPa and 400-500 MPa
 837 regions for *Y. enterocolitica* inactivation in phosphate buffer and milk,
 838 respectively, so the mean value of n was applied for each pressure range. However
 839 the former assumption that n is pressure independent was not valid for the entire
 840 experimental pressure range (300-500 MPa). On the contrary, Doona et al. (2008)
 841 and Buzrul and Alpas (2004) observed concavity changes (Table 2), where n
 842 tended to increase with processing pressure temperature. Therefore, a constant
 843 $n(T)$ or $n(P)$ may not be the reflect of a non-significant pressure and/or
 844 temperature effect on the kinetic model parameters, but a consequence of the

845 narrow pressure and temperature ranges under which the experiments were
 846 performed. The pressure-dependence of the shape parameter, $n(P)$, can be
 847 calculated empirically, e.g., using the model proposed by Pilavtepe-Çelik et al.
 848 (2009) for the inactivation of pathogens in carrot juice and peptone water (Eq.
 849 85). The exponential model describing $P_c(T)$ and $T_c(P)$ (Eq. 81-82) can also be
 850 applied to the model parameter $n(T)$ or $n(P)$ (Eq. 86-87) (Doona et al., 2008).

$$n(P) = n_{ref} + a \cdot \left(\frac{1}{P} - \frac{1}{P_{ref}} \right) \quad (85)$$

$$n(P) = d_{0P}(T) \cdot \exp[-d_{1P}(T) \cdot P] \quad (86)$$

$$n(T) = d_{0T}(P) \cdot \exp[-d_{1T}(P) \cdot T] \quad (87)$$

851
 852 Recently Carreño et al. (2011) proposed an alternative Weibull secondary model
 853 for the survival fraction ($\log_{10} S$) under isothermal and isobaric conditions by
 854 inferring that the pressure and temperature resistance of microorganisms followed
 855 a Weibull distribution. Pressure and temperature substituted the independent
 856 variable time (t) in Eq. 9 and resulted in Eq. 88-89.

$$S(P) = -\left(\frac{P}{f_P} \right)^n \quad (88)$$

$$S(T) = -\left(\frac{T}{f_T} \right)^n \quad (89)$$

857
 858 The parameters f_P and f_T represent the pressure and temperature for the first
 859 decimal reduction of the microbial population. The use of the isothermal model to
 860 describe the inactivation of *L. plantarum* at 0-400 MPa for 10-60 s in tangerine
 861 juice with an initial temperature of 15-45°C yielded $R^2 = 0.952-0.990$ and A_f
 862 $= 1.021-1.066$ (Carreño et al., 2011). Although no sigmoidal curves were
 863 observed, Carreño et al. (2011) also investigated the kinetics of *L. plantarum* HPP
 864 inactivation combined with mild heat treatments (45-90°C, 10 s). The survival
 865 curves presented concavity changes and the single Weibull model with pressure
 866 and temperature as independent variables (Eq. 88-89) had an inaccurate fit (36%
 867 prediction error). As a result, a biphasic Weibull model (Eq. 90) combining Eq. 15
 868 and Eq. 88 was applied and yielded a 9% prediction error with $A_f = 1.009$.

$$N(T) = \frac{N_0}{1 + 10^\Psi} \left[10^{\left[\Psi \left(\frac{T}{f_{T1}} \right)^{n1} \right]} + 10^{\left(\frac{T}{f_{T2}} \right)^{n2}} \right] \quad (90)$$

869

870 For isothermal conditions, Eq. 79 can also be expressed as a function of the
871 pressure applied (Eq. 91)

$$N(P) = \frac{N_0}{1 + 10^\Psi} \left[10^{\left[\Psi \left(\frac{P}{f_{P1}} \right)^{n1} \right]} + 10^{\left(\frac{P}{f_{P2}} \right)^{n1}} \right] \quad (91)$$

872

873 Finally, it is important to note that information concerning any of the Weibull
874 HPP secondary models here presented is scarce (Table 7).

875

876 INSERT TABLE 7

877 **Simultaneous pressure and temperature effects on quasi-chemical**
878 **kinetic model parameters**

879 Only Doona et al. (2008) have reported secondary inactivation expressions for the
880 quasi-chemical kinetic model. This includes a general inactivation rate constant
881 (μ) for *E. coli* (207-345 MPa, 30-50°C) as the minimum slope of the process
882 lethality $L(t)$ (Eq. 93). The time at which μ occurs can be defined as t_μ ($t = t_\mu$),
883 thus $L_\mu = L(t_\mu)$, and the initial phase of the HPP for which no microbial
884 inactivation occurs is defined as the “lag time” ($L_0 = 0$; $t = \lambda$). A straight line of
885 $L(t)$ with slope μ can be observed from L_0 to L_μ as in Eq. 93, and the lag time can
886 be obtained by solving for λ , which is a function of the total microbial plate counts
887 (U) determined experimentally as shown in Eq. 92 .

$$\mu = \frac{L_\mu - L_0}{t_\mu - \lambda} \quad (92)$$

$$L(t) = \frac{d \log_{10}(U(t))}{dt} \quad (93)$$

$$U(t) = M^* + M^{**}$$

$$\mu = \frac{L_\mu - L_0}{t_\mu - \lambda} \quad (93)$$

888

889 The pressure dependence of the inactivation rate μ for *E. coli* under isothermal
890 conditions (30-50°C) showed a log-linear relationship. Furthermore, Doona et al.
891 (2008) fitted the experimental data to Eq. 94 to describe the pressure-temperature
892 effect on the kinetic constant $\mu(P,T)$. The coefficient values $C_0 = 4.496 \pm 0.2007$,
893 $C_T = -0.0416 \pm 0.0038$, and $C_P = -0.0417 \pm 0.0028$ are valid only when pressure is
894 expressed in *psi* units, but the model behavior was acceptable in the entire
895 experimental range as observed in Fig. 8a ($R^2 = 0.956$).

$$-\log_{10} \mu(P,T) = C_0 + C_T \cdot T + C_P \cdot P \quad (94)$$

896
897 The application of this secondary model was extended to predict the time (t_p)
898 required for 6 decimal reductions in *E. coli* counts for various pressure and
899 temperature combinations. The extended model (Eq. 95) also included the lag
900 time (λ), and the predicted processing times to achieve $\log N/N_0 = -6$ (t_p) were
901 consistent with a new set of experimental conditions that were selected for
902 validation (Fig. 8b).

$$t_p = \lambda + \frac{6}{\mu(P,T)} \quad (95)$$

903
904 Secondary models for the enhanced quasi chemical kinetic model (EQCKM) were
905 semi-empirical equations based on the Eyring and Arrhenius model, which were
906 discussed in the section describing the EQCKM model.

907

908 INSERT FIGURE 8

909 **Simultaneous pressure and temperature effects on kinetics models** 910 **under dynamic conditions**

911 During PATP, the difference in thermophysical and transport properties, and
912 several PATP design variables (inlet fluid, vessel design, location of food samples
913 in the pressure chamber, food product composition and geometry, etc.) affect
914 temperature, leading to heat transfer between the food, pressurizing fluid, vessel
915 walls and equipment surroundings (Denys et al., 2000; Hartmann and Delgado,
916 2002, 2003; Otero et al., 2007; Barbosa-Cánovas and Juliano, 2008; Infante et al.,
917 2009; Knoerzer et al., 2011). Therefore, isothermal conditions are difficult to
918 achieve even for lab-scale PATP units, influencing the interpretation and validity

919 of experimental observations. Experimental practices to approach quasi-adiabatic
920 PATP conditions include: (a) isolate the sample and pressurizing fluid in a carrier
921 with low thermal conductivity (de Heij et al., 2003; Van Scepdael et al., 2004;
922 Wang et al., 2009; Grauwet et al., 2010; Ramaswamy et al., 2010; Shao et al.,
923 2010; Daryaei and Balasubramaniam, 2013); (b) reduce the pressurization rate
924 allowing more time to dissipate adiabatic heating; (c) start the kinetic study after
925 thermal equilibrium is achieved (Ly-Nguyen et al., 2003; Van Opstal et al., 2005;
926 Verlinde et al., 2009; Ghawi et al., 2012); and, (d) use dynamic kinetics modeling
927 techniques to interpret the data (Ludikhuyze et al., 1997a; Ludikhuyze et al.,
928 1998a; Peleg et al., 2012). However, these experimental approaches do not solve
929 the need to incorporate the dynamic temperature conditions in the design of PATP
930 process meeting desired safety and quality objectives. Therefore, fluid dynamics
931 simulation under PATP conditions *is a must* and numerous authors had made
932 important contributions in this field. However, an in depth coverage of studies
933 also is beyond the scope of the current review, thus just a few examples will be
934 examined next.

935

936 ***Dynamic Eyring-Arrhenius model***

937 Ludikhuyze et al. (1997a) demonstrated that non-isobaric and non-isothermal
938 conditions affected the predicted values of *Bacillus subtilis* α -amylase inactivation
939 in Tris-HCl buffer (0.01 M, pH 8.6) and in a buffer-water-glycerol (15% w/w)
940 mix. A secondary model that described the pressure and temperature dependence
941 of the first order kinetics rate constant (k) was previously obtained under uniform
942 pressure-temperature conditions (Eq. 96) and tested for dynamic PATP treatments
943 (Eq. 97) (Ludikhuyze et al., 1997b). The secondary inactivation model developed
944 under static pressure-temperature conditions clearly underestimated dynamic P-T
945 effects and Eq. 96 parameters had to be recalculated. A new set of secondary
946 model parameters was obtained by coupling residual activity with the
947 corresponding pressure-temperature profiles, accurately predicting α -amylase
948 inactivation for both static and dynamic PATP conditions ($R^2 = 0.95-0.98$).
949 Additionally, the authors attempted to obtain a model combining both static and
950 dynamic enzymatic kinetic data although the predictions registered an error
951 between 5% and over 100% (Ludikhuyze et al., 1997a). Likewise, Ludikhuyze et

952 al. (1998a) came upon the same situation when validating another empirical
 953 secondary model (Eq. 55) for soybean lipoxygenase (LOX) inactivation at 0.1-650
 954 MPa, 10-64°C).

$$k(P, T) = k_0 \cdot \exp \left\{ - \left[B \cdot \left(\frac{1}{T} - \frac{1}{T_0} \right) + C \cdot (P - P_0) \right] \right\} \quad (96)$$

$$\ln \frac{A}{A_0} = \int_0^t k(P, T) \cdot dt \quad (97)$$

955

956 **3-Endpoints Method**

957 Envisioning PATP inactivation kinetics as a purely dynamic thermal process
 958 based on the 3-Endpoints method was recently proposed by Peleg et al. (2012).
 959 Measuring microbial counts and other intrinsic properties without interrupting the
 960 food treatment is not always possible. For example, a multiple vessel system run,
 961 or multiple runs with various holding times when using a single vessel system, are
 962 required to determine the kinetic effects of HPP treatments. In the case of thermal
 963 treatments, the capillary method cannot be applied for solid food matrixes and the
 964 withdrawal of samples is practically impossible (Corradini et al., 2009; Peleg et
 965 al., 2012). The 3-Endpoints method allows the estimation of inactivation model
 966 parameters using the final survival ratios ($\log_{10} S$) and their respective temperature
 967 profiles (Corradini et al., 2009). A dynamic Weibull model $\log S[T(t)]$ (Eq. 98)
 968 can be obtained as described in the following paragraphs (Peleg et al., 2005;
 969 Peleg, 2006).

$$\frac{d \log_{10} S(t)}{dt} = -b'[T(t)] \cdot n[T(t)] \cdot \left\{ - \frac{\log_{10} S(t)}{b'[T(t)]} \right\}^{\frac{n[T(t)]-1}{n[T(t)]}} \quad (98)$$

970

971 An equation describing the dynamic changes in the microbial population
 972 ($S = \log N/N_0$) can be obtained by calculating the derivative of the Weibull kinetic
 973 model (Eq. 9). The process temperature can briefly assumed to remain constant at
 974 $t = t^*$ (Eq. 99-100). Thus, the slope at $t = t^*$ is equal to the instantaneous surviving
 975 population (Fig. 9), and by substituting Eq. 100 in Eq. 99 the dynamic Weibull
 976 kinetic model is obtained (Eq. 98).

977

$$\left| \frac{d \log_{10} S(t)}{dt} \right|_T = -b'(T) \cdot n(T) \cdot t^{n(T)-1} \quad (99)$$

$$t^* = \left\{ -\frac{\log_{10} S(t)}{b[T(t)]} \right\}^{\frac{1}{n(T)}} \quad (100)$$

978

979 INSERT FIGURE 9

980

981 The logistic model for $b'(T)$ described by Eq. 79 was incorporated in the dynamic
 982 Weibull model (Eq. 98) by Peleg (2012). If temperature has no effect on the shape
 983 parameter n , three final survival ratios (S_1, S_2, S_3) and three temperature profiles
 984 (T_1, T_2, T_3) are needed (Fig. 10) to formulate a 3 x 3 differential equation system
 985 whose solution will yield the dynamic Weibull model parameters n, w_c and T_c
 986 (Corradini et al., 2009). However, Peleg et al. (2012) highlighted the model
 987 impracticality when the pressure dependence of b' is incorporated (Eq. 80), and
 988 the difficulties to numerically solve the differential equation system when n can
 989 no longer be considered constant in the temperature and pressure range of interest.

990

991 INSERT FIGURE 10

992 Final Remarks

993 At present, the availability of kinetics model and data for the pressure processing
 994 of foods is still very limiting, inconsistent, and lagging behind the standardized
 995 information available for food pasteurization and sterilization by conventional
 996 thermal treatments. Parameters describing the microbial inactivation kinetics have
 997 been determined mostly only for the primary models most frequently utilized in
 998 thermal food processing, i.e., first order kinetics, Weibull and log-logistic models,
 999 whereas the Bigelow model is still the only one generally used for secondary
 1000 modeling. Applications of non-linear models such as the Weibull and log-logistic
 1001 equations, frequently used to describe the non-linear behavior observed typically
 1002 in the pressure inactivation of enzymes, were not found.

1003

1004 Although a large number of empirical and phenomenological secondary models
 1005 predicting pressure and temperature effects on the inactivation rate constant for

1006 the pressure-inactivation of enzymes and microorganisms were found and are
1007 presented in this review, no general model has been developed. This may reflect
1008 the complexity of the kinetics of inactivation by pressure and the insufficiency of
1009 good-quality experimental data. Since narrow experimental ranges were
1010 consistently observed in the literature reviewed, extreme caution is recommended.
1011 The limited number of experimental conditions considered in these experiments
1012 may lead to the misinterpretation of results. Thus, kinetic studies covering 600
1013 MPa pressure and 50°C temperature intervals, respectively, appear sufficient
1014 when evaluating the inactivation kinetics of most moderate- and high-
1015 pressure/temperature resistant microorganisms and enzymes. Moreover, the
1016 increasing availability of mathematical tools, computer software and high pressure
1017 equipment instrumentation has motivated researchers to increase the amount of
1018 dynamic kinetic model data since knowledge of the temperature gradients
1019 generated within the vessel is crucial for the assessment of PATP/PATS
1020 applications.

1021

1022 **ACKNOWLEDGEMENT**

1023 The authors acknowledge the support from the Tecnológico de Monterrey
1024 (Research chair funds CAT 200), México's CONACYT Scholarship Program, and
1025 Formula Grants no. 2011-31200-06041 and 2012-31200-06041 from the USDA
1026 National Institute of Food and Agriculture.

1027

Table 1. Reported values for the first order inactivation related kinetics and related models

Target	Medium	Pressure Come Up Time Holding time Depressurization Temperature	Kinetic model	Model parameters	Regression software	Reference
Aerobic bacteria	Fresh, whole, raw milk pH 6.64 7.68 x 10 ⁷ cfu ml ⁻¹ inoculum	300, 400, 600 MPa 100-200 MPa s ⁻¹ 0-105 min NR 25°C	First order (Eq. 3) <i>D</i> value (Eq. 4)	$k = 0.1643-0.7576 \text{ min}^{-1}$ $D_p = 3.04-14.03 \text{ min}$	SigmaPlot 8.0	(Dogan and Erkmen, 2004)
Aerobic bacteria	Fresh, filtered orange juice pH 3.35 5.71 x 10 ⁷ cfu ml ⁻¹ inoculum	300, 400, 600 MPa 100-200 MPa s ⁻¹ 0-30 min NR 25°C	First order (Eq. 3) <i>D</i> value (Eq. 4)	$k = 0.5152-1.8573 \text{ min}^{-1}$ $D_p = 1.24-4.47 \text{ min}$	SigmaPlot 8.0	(Dogan and Erkmen, 2004)
Aerobic bacteria	Fresh, filtered peach juice pH 5.21 5.75 x 10 ⁷ cfu ml ⁻¹ inoculum	300, 400, 600 MPa 100-200 MPa s ⁻¹ 0-70 min NR 25°C	First order (Eq. 3) <i>D</i> value (Eq. 4)	$k = 0.2357-1.0812 \text{ min}^{-1}$ $D_p = 2.13-9.77 \text{ min}$	SigmaPlot 8.0	(Dogan and Erkmen, 2004)

Aerobic bacterial spores	Deionized water	700 MPa	<i>D</i> value (Eq. 4)	$D_p = 0.30-0.60$ min (105°C) $D_p = 0.10-0.50$ min (121°C)	Microcal Origin 7.5	(Ahn et al., 2007)
	<i>B. amyloliquefaciens</i> TMW 2.479	0.58 min				
	Fad 82	0-5 min				
	<i>B. amyloliquefaciens</i> TMW 2.482	NR				
	Fad 11/2	105, 121°C				
	<i>B. sphaericus</i> NZ 14 <i>B. amyloliquefaciens</i> ATCC 49763					
Anaerobic bacterial spores	Deionized water	700 MPa	<i>D</i> value (Eq. 4)	$D_p = 0.20-0.60$ min (105°C) $D_p = 0.30$ min (121°C)	Microcal Origin 7.5	(Ahn et al., 2007)
	<i>C. sporogenes</i> ATCC 7955	0.58 min				
	<i>C. tyrobutylicum</i> ATCC 27384 <i>T. thermosaccharolyticum</i> ATCC 27384	0-5 min NR 105, 121°C				
<i>Bacillus stearothermophilus</i> spores	Egg	400, 600, 700 MPa	<i>D</i> value (Eq. 4)	$D_p = 0.41-0.72$ min	SAS	(Rajan et al., 2006)
	Defrosted egg patties	1.9-2.4 min				
	10^6 spores g ⁻¹ inoculum	0-16 min NR 105.8±0.6°C				
<i>Escherichia coli</i>	Fresh extracted carrot juice	200, 250, 300, 350, 400, 450,	<i>D</i> value (Eq. 4)	$D_p = 2.00-188.00$ min	SAS online DOC 8.01	(Van Opstal et al., 2005)
	pH 6.6	500, 550, 600 MPa				
	K-12 strain MG1655	100 MPa min ⁻¹				
	10^9 cfu ml ⁻¹ inoculum	0-60 min NR 5-45°C				

<i>Listeria monocytogenes</i>	Fresh, whole, raw milk	300, 400, 600 MPa	First order (Eq. 3)	$k = 0.2096-0.9477 \text{ min}^{-1}$	SigmaPlot 8.0	(Dogan and Erkmen, 2004)
	pH 6.64 7.48 x 10 ⁷ cfu ml ⁻¹ inoculum	100-200 MPa s ⁻¹ 0-105 min NR 25°C	<i>D</i> value (Eq. 4)	$D_p = 2.43-10.99 \text{ min}$		
<i>Listeria monocytogenes</i>	Fresh, filtered orange juice	300, 400, 600 MPa	First order (Eq. 3)	$k = 0.8024-2.6471 \text{ min}^{-1}$	SigmaPlot 8.0	(Dogan and Erkmen, 2004)
	pH 3.35 2.93 x 10 ⁷ cfu ml ⁻¹ inoculum	100-200 MPa s ⁻¹ 0-30 min NR 25°C	<i>D</i> value (Eq. 4)	$D_p = 0.87-2.87 \text{ min}$		
<i>Listeria monocytogenes</i>	Fresh, filtered peach juice	300, 400, 600 MPa	First order (Eq. 3)	$k = 0.3733-1.5151 \text{ min}^{-1}$	SigmaPlot 8.0	(Dogan and Erkmen, 2004)
	pH 5.21 2.95 x 10 ⁷ cfu ml ⁻¹ inoculum	100-200 MPa s ⁻¹ 0-70 min NR 25°C	<i>D</i> value (Eq. 4)	$D_p = 1.52-6.17 \text{ min}$		
Native microflora	Unpasteurized Hamlin variety orange juice pH 3.7, 10.7°Brix	350, 400, 450, 500 MPa 45-60 s 1-300 s NR 25±5°C	First order (Eq. 3) <i>D</i> value (Eq. 4)	$k = 0.0002-0.0064 \text{ min}^{-1}$ $D_p = 0.05-1.32 \text{ min}$	NR	(Parish, 1998)

<i>Saccharomyces cerevisiae</i>	Commercial pasteurized orange juice	350, 400, 450, 500 MPa 45-60 s	First order (Eq. 3) <i>D</i> value (Eq. 4)	$k = 0.0002-0.041 \text{ min}^{-1}$ $D_p = 0.07-1.27 \text{ min}$	NR	(Parish, 1998)
ascospores	10^5 cfu ml^{-1} inoculum	1-300 s NR 25±5°C				
<i>Saccharomyces cerevisiae</i>	Commercial pasteurized orange juice	350, 400, 450, 500 MPa 45-60 s	First order (Eq. 3) <i>D</i> value (Eq. 4)	$k = 0.0005-0.0137 \text{ min}^{-1}$ $D_p = 0.02-0.63 \text{ min}$	NR	(Parish, 1998)
vegetative cells	10^5 cfu ml^{-1} inoculum Several strains	1-300 s NR 25±5°C				
<i>Vibrio cholerae</i>	Phosphate-buffered saline 10^8 cfu ml^{-1} inoculum Several strains	200-250 MPa 55-80 s 0-240 s <2 s 8-10°C (initial)	<i>D</i> value (Eq. 4)	$D_p = 2.10-3.38 \text{ min}$ (200 MPa) $D_p = 0.60-0.82 \text{ min}$ (250 MPa)	Microsoft Excel	(Cook, 2003)
<i>Vibrio parahaemolyticus</i>	Phosphate-buffered saline 10^8 cfu ml^{-1} inoculum Several strains	200-250 MPa 55-80 s 0-240 s <2 s 8-10°C (initial)	<i>D</i> value (Eq. 4)	$D_p = 0.88-2.78 \text{ min}$ (200 MPa) $D_p = 0.26-0.60 \text{ min}$ (250 MPa)	Microsoft Excel	(Cook, 2003)

<i>Vibrio vulnificus</i>	Phosphate-buffered saline 10 ⁸ cfu ml ⁻¹ inoculum Several strains	200-250 MPa 55-80 s 0-240 s <2 s 8-10°C (initial)	<i>D</i> value (Eq. 4)	<i>D_p</i> = 0.28-0.62 min (200 MPa)	Microsoft Excel	(Cook, 2003)
--------------------------	---	---	------------------------	--	-----------------	--------------

Table 2. Reported parameters for the primary Weibull model describing HPP inactivation kinetics.

Target	Medium	Pressure	Model parameters	Regression software	Reference
		Come Up Time Holding time Depressurization Temperature			
Aerobic bacterial spores	Deionized water	700 MPa	$b' = 1.5-3.1$ (105°C); 2.1-6.5 (121°C)	Microcal Origin 7.5	(Ahn et al., 2007)
	<i>B. amyloliquefaciens</i> TMW 2.479 Fad 82	0.58 min	$n = 0.2-0.5$ (105°C); 0.3-1.0 (121°C)		
	<i>B. amyloliquefaciens</i> TMW 2.482 Fad 11/2	0-5 min			
	<i>B. sphaericus</i> NZ 14	NR			
Anaerobic bacterial spores	Deionized water	700 MPa	$b' = 1.5-3.2$ (105°C); 1.7-2.8 (121°C)	Microcal Origin 7.5	(Ahn et al., 2007)
	<i>C. sporogenes</i> ATCC 7955	0.58 min	$n = 0.2-0.5$ (105°C); 0.5-0.7 (121°C)		
	<i>C. tyrobutylicum</i> ATCC 27384	0-5 min			
	<i>T. thermosaccharolyticum</i> ATCC 27384	NR			
<i>Bacillus coagulans</i> spores	Phosphate buffer (100 mM, pH 6.7)	400-600MPa	$b' = 1.977-2.622$ (70°C); 1.553-3.447 (80°C)	SPSS 13.0	(Wang et al., 2009)
	10 ⁶ cfu ml ⁻¹ inoculum	3.1-4.6 min	$n = 0.160-0.207$ (70°C); 0.124-0.260 (80°C)		
	IFFI 10144 strain	0-30 min			
		NR			
		70-80°C (initial temperature)			

<i>Bacillus</i> <i>stearothermophilus</i> spores	Egg Defrost egg patties 10 ⁶ spores g ⁻¹ inoculum	400, 600, 700 MPa 1.9-2.4 min 0-16 min NR 105.8±0.6°C	$b' = 1.30-1.96$ $n = 0.30-0.54$	SAS	(Rajan et al., 2006)
<i>Escherichia coli</i>	Whey protein surrogate food system ATCC 11229 strain	207-439 MPa NR 0-300 min NR 30, 40, 50 °C	$b' = 2.7 \times 10^{-8} - 0.482$ (30°C); $4.0 \times 10^{-4} - 2.161$ (40°C); $3.0 \times 10^{-3} - 2.653$ (50°C) $n = 0.70-3.37$ (30°C); $0.36-2.24$ (40°C); $0.48-1.81$ (50°C)	NR	(Doona et al., 2008)
<i>Escherichia coli</i>	UHT whole milk pH 6.64 10 ⁸ cfu ml ⁻¹ inoculum ATCC 11775 strain	400, 450, 500, 550, 600 MPa 300 MPa min ⁻¹ 0-80 min 300 MPa min ⁻¹ 22°C	$b' = 1.2-10.5$ $n = 0.78$	SigmaPlot 2000 6.0	(Buzrul et al., 2008)
<i>Listeria innocua</i>	UHT whole milk pH 6.64 10 ⁸ cfu ml ⁻¹ inoculum ATCC 33090 strain	400, 450, 500, 550, 600 MPa 300 MPa min ⁻¹ 0-80 min 300 MPa min ⁻¹ 22°C	$b' = 1.1-12.2$ $n = 0.79$	SigmaPlot 2000 6.0	(Buzrul et al., 2008)

<i>Listeria innocua</i>	Peptone solution 0.1% CDW47 strain 10 ⁸ -10 ⁹ cfu ml ⁻¹ inoculum	138, 207, 276, 345 MPa 300 MPa min ⁻¹ 0-30 min <1 min 25, 35, 45, 50°C	$b' = 0.09-0.21$ (25°C); $0.01-0.03$ (35°C); $0.002-2.12$ (45°C); $0.19-4.38$ (50°C) $n = 0.45-0.79$ (25°C); $0.64-1.26$ (35°C); $0.35-1.87$ (45°C); $0.23-1.14$ (50°C)	SigmaPlot 2000 6.0	(Buzrul and Alpas, 2004)
<i>Yersinia enterocolitica</i>	UHT whole milk pH 6.70 5 x 10 ⁸ cfu ml ⁻¹ inoculum ATCC 35669 strain	400-500 MPa	$b' = 0.66$ (400 MPa); 1.13 (500 MPa) *Calculated from linear approach $n = 0.583$	SAS 8.2	(Chen and Hoover, 2003a)

Table 3. Reported parameters for the primary log-logistic model describing HPP inactivation kinetics.

Target	Medium	Pressure	Kinetic model	Model parameters	Regression software	Reference
		Come Up Time Holding time Depressurization Temperature				
<i>Bacillus coagulans</i> spores	Phosphate buffer 100 mM, pH 6.7 10 ⁶ cfu ml ⁻¹ inoculum IFFI 10144 strain	400-600MPa	3 parameter (Eq. 23)	$H = -(4.611-18.848) 70^{\circ}\text{C}$	SPSS 13.0	(Wang et al., 2009)
		3.1-4.6 min		$H = -(4.754-5.938) 80^{\circ}\text{C}$		
		0-30 min		$\Omega = -(1.871-2.074) 70^{\circ}\text{C}$		
		NR		$\Omega = -(1.726-2.953) 80^{\circ}\text{C}$		
		70-80°C (initial temperature)		$\tau = 0.449-3.956 (70^{\circ}\text{C})$		
				$\tau = 0.011-1.049 (80^{\circ}\text{C})$		
<i>Listeria innocua</i>	Peptone solution 0.1% CDW47 strain 10 ⁸ -10 ⁹ cfu ml ⁻¹ inoculum	138, 207, 276, 345 MPa	3 parameter (Eq. 23)	$H = -(4.92-23.39) 25^{\circ}\text{C}$	SigmaPlot 2000 6.0	(Buzrul and Alpas, 2004)
		300 MPa min ⁻¹		$H = -(2.89-15.08) 35^{\circ}\text{C}$		
		0-30 min		$H = -(1.26-56.24) 45^{\circ}\text{C}$		
		<1 min		$H = -(1.37-39.71) 50^{\circ}\text{C}$		
		25, 35, 45, 50°C		$\Omega = \text{NR}$		
				$\tau = \text{NR}$		

<i>Yersinia enterocolitica</i>	UHT whole milk pH 6.70 5×10^8 cfu ml ⁻¹ inoculum ATCC 35669 strain	350-500 MPa	3 parameter (Eq. 23)	$H = -(9.878-27.884)$ $\Omega = -(7.748-11.199)$ $\tau = 1.478-2.100$	SAS 8.2	(Chen and Hoover, 2003a)
<i>Yersinia enterocolitica</i>	UHT whole milk pH 6.70 5×10^8 cfu ml ⁻¹ inoculum ATCC 35669 strain	350-500 MPa	2 parameter (Eq. 24)	$H = -14$ $\Omega = -(6.944-10.324)$ $\tau = 1.380-1.989$	SAS 8.2	(Chen and Hoover, 2003a)

Table 4. Reported parameters for an attempted global Bigelow secondary model. Modified from Santillana Farakos and Zwietering (2011).

Microorganism	<i>D</i> samples	<i>P</i> range (MPa)	<i>T</i> range (°C)	R^2_{adj}	z_P	z_T	$\log D_{PrefTref}$	P_{ref} (MPa)	T_{ref} (°C)
<i>Bacillus</i> spp. spores	48	100-700	45-121	0.86	614.7±122.9	45.2±6.5	0.27±0.25	400	100
<i>Clostridium</i> spp. spores	54	600-900	80-121	0.88	616.3±106.3	20.4±1.1	0.85±0.36	400	100
<i>Cronobacter</i> spp.	24	200-600	22-25	0.78	368.2±39.4	NR	-0.19±0.13	400	NR
<i>Escherichia coli</i>	117	100-700	2-50	0.30	385.6±53.2	97.5±45.2	0.88±0.23	400	30
<i>Listeria</i> spp.	74	200-700	2-50	0.61	298.9±34.6	38.6±7.5	0.56±0.18	400	30
<i>Vibrio</i> spp.	80	69-345	10-25	0.61	206.9±32.0	-18.4±2.3	0.06±0.20	400	30
<i>Zygosaccharomyces bailii</i>	48	100-400	-5-45	0.71	91.0±8.4	141-7±58.6	-0.84±0.24	400	30

Table 5, Reported parameters for the secondary Eyring-Arrhenius related models and its variants.

Target	Medium	Pressure	Kinetic model	Model parameters	Regression software	Reference
		Come Up Time				
		Holding time				
		Depressurization				
		Temperature				
Alkaline phosphatase	Bovine milk	0.1-725 MPa	Decimal reduction time empirical model (Eq. 72)	$c_1 = 3.33 \pm 0.16$	SAS	(Ludikhuyze et al., 2000)
		100 MPa min ⁻¹		$c_2 = (3.88 \pm 0.77) * 10^{-3}$		
		14-300 min		$c_3 = (-1.05 \pm 0.09) * 10^{-5}$		
		NR		$c_4 = 4.88 \pm 0.02$		
		25-63°C		$c_5 = (5.3 \pm 0.90) * 10^{-2}$		
				$c_6 = (-2.7 \pm 0.7) * 10^{-8}$		
				$T_{ref} = 323 \text{ K}$		
<i>Lactobacillus brevis</i>	Orange juice Greek Valencia variety pH 3.8, 11.6°Brix	100-500 MPa	Eyring-Arrhenius decimal reduction times (Eq. 68)	$D_{ref,P,T} = 3.42 \pm 0.51 \text{ min}^{-1}$	SYSTAT 8.0 Least squares regression analysis	(Katsaros et al., 2010)
		NR		$P_{ref} = 300 \text{ MPa}$		
		0-30 min		$T_{ref} = 303 \text{ K}$		
		NR		$z_T = 23.8 \pm 1.4 \text{ °C}$		
		20-40°C		$z_P = 94.7 \pm 7.8 \text{ MPa}$		
				$a = -0.009 \pm 0.001 \text{ MPa}^{-1}$		

<i>Lactobacillus plantarum</i>	Orange juice Greek Valencia variety pH 3.8, 11.6°Brix	100-500 MPa NR 0-30 min NR 20-40°C	Eyring-Arrhenius decimal reduction times (Eq. 68)	$D_{refP,T} = 1.32 \pm 0.11 \text{ min}^{-1}$ $P_{ref} = 300 \text{ MPa}$ $T_{ref} = 303 \text{ K}$ $z_T = 18.8 \pm 1.3 \text{ }^\circ\text{C}$ $z_P = 95.0 \pm 11 \text{ MPa}$ $a = -0.013 \pm 0.002 \text{ MPa}^{-1}$	SYSTAT 8.0 Least squares regression analysis	(Katsaros et al., 2010)
Lipoxygenase (LOX)	Tris-HCl buffer (0.01 M, pH 9) Commercial lyophilized soybean type B LOX	50-650 MPa 100 MPa min ⁻¹ NR NR 10-64°C	Empirical Eyring Arrhenius (Eq. 55)	$c_1 = -3.12 \pm 0.28$ $c_2 = (-1.39 \pm 0.18) * 10^{-1}$ $c_3 = (2.66 \pm 0.27) * 10^{-3}$ $c_4 = -15.6 \pm 1.4$ $c_5 = (7.1 \pm 0.28) * 10^{-2}$	SAS	(Ludikhuyze et al., 1998b, a)
Pectinmethylesterase (PME)	Orange juice Greek Valencia variety pH 3.8, 11.6°Brix	100-500 MPa NR 0-30 min NR 20-40°C	Eyring-Arrhenius (Eq. 47)	$k_{refP,T} = 0.582 \pm 0.048 \text{ min}^{-1}$ $P_{ref} = 300 \text{ MPa}$ $T_{ref} = 308 \text{ K}$ $E_{aP} = 95 \pm 11 \text{ KJ mol}^{-1}$ $V_T^\ddagger = -30 \pm 5 \text{ cm}^3 \text{ mol}^{-1}$ $a = 0.64 \pm 0.07 \text{ cm}^3 \text{ mol}^{-1} \text{ K}^{-1}$ $g = -0.002 \pm 0.0003 \text{ MPa}^{-1}$	SYSTAT 8.0 Least squares regression analysis	(Katsaros et al., 2010)

Pectinmethylesterase (PME)	Orange juice Navel variety (<i>Citrus sinensis</i>)	100-800 MPa NR 0-30 min NR 30-60°C	Eyring-Arrhenius (Eq. 47)	$k_{ref,P,T} = 1.76 \text{ min}^{-1}$ $P_{ref} = 600 \text{ MPa}$ $T_{ref} = 323 \text{ K}$ $E_{aP} = 148 \text{ KJ/mol}$ $V_T^\ddagger = -25.1 \text{ cm}^3 \text{ mol}^{-1}$ $a = 0.703 \text{ cm}^3 \text{ mol}^{-1} \text{ K}^{-1}$ $g = 8.374 \times 10^{-4} \text{ MPa}^{-1}$ * Valid in 40-60°C range only due to enzyme reactivation at $T < 40^\circ\text{C}$	SYSTAT	(Polydera et al., 2004)
Pectinmethylesterase (PME)	Deionized water (pH 4.5) Commercial orange peel PME 0.4 mg PME powder per ml of buffer	50-900 MPa NR 20-220 min NR 15-82°C	Empirical Eyring Arrhenius (Eq. 52)	$c_1 = -1.88 \pm 0.10$ $c_2 = (-17.55 \pm 1.09) * 10^{-3}$ $c_3 = (53.27 \pm 3.26) * 10^{-6}$ $c_4 = (-35.95 \pm 2.79) * 10^{-9}$ $c_5 = 352.12 \pm 18.55$ $c_6 = 0.348 \pm 0.027$	NR	(Van den Broeck et al., 2000)
Pectinmethylesterase (PME)	Citric acid buffer 5 mM, pH 3.7 Lyophilized orange pulp PME extract Navel variety 2.0 mg PME powder per ml of buffer	50-900 MPa NR 20-220 min NR 15-82°C	Empirical Eyring Arrhenius (Eq. 52)	$c_1 = -2.39 \pm 0.17$ $c_2 = (-19.00 \pm 1.83) * 10^{-3}$ $c_3 = (55.20 \pm 5.94) * 10^{-6}$ $c_4 = (-38.50 \pm 5.35) * 10^{-9}$ $c_5 = 193.44 \pm 22.89$ $c_6 = 0.248 \pm 0.036$	NR	(Van den Broeck et al., 2000)

Polyphenoloxidase (PPO)	Phosphate buffer (pH 7; 0.1 M)	0.1-900 MPa	Empirical Eyring Arrhenius (Eq. 51)	$c_1 = -2.42 \pm 0.07$ $c_2 = (-17.2 \pm 0.7) * 10^{-3}$ $c_3 = (41.1 \pm 1.8) * 10^{-6}$ $c_4 = (-23.3 \pm 1.3) * 10^{-9}$ $c_5 = (-16.8 \pm 0.6) * 10^{-4}$ $E_{aP} = 342.30 \pm 11.63 \text{ KJ mol}^{-1}$	NR	(Weemaes et al., 1998b)
	Lyophilized avocado PPO powder 0.5 mg PPO powder per ml of buffer	NR 35-180 min NR 25-77.5°C				
<i>Saccharomyces cerevisiae</i>	0.85% NaCl solution	120-300 MPa	Quadratic model (Eq. 70)	$c_1 = -4.26$ $c_2 = 1.25 * 10^{-2}$ $c_3 = -3.37 * 10^{-2}$ $c_4 = 8.55 * 10^{-6}$ $c_5 = -7.55 * 10^{-5}$ $c_6 = 1.42 * 10^{-3}$ $P_{ref} = 0.1 \text{ MPa}$ $T_{ref} = 273 \text{ K}$	NR	(Hashizume et al., 1995)
	8.0 x 10 ⁶ -1.0 x 10 ⁷ cfu ml ⁻¹ inoculum at stationary phase IFO 0234 strain	2 min 0-40 min 30 s (-20)-50°C				
<i>Zygosaccharomyces bailii</i>	Tris-HCl buffer 40mM, pH 6.5 CBS 109	120-320 MPa 100 MPa min ⁻¹ 0-60 min NR (-5)-45°C	Reduced Quadratic model (Eq. 71)	$c_1 = 1.55 \pm 0.04$ $c_2 = -(15.05 \pm 0.49) * 10^{-3}$ $c_3 = -(24.05 \pm 1.53) * 10^{-3}$ $c_4 = (23.52 \pm 6.63) * 10^{-6}$ $c_5 = -(16.42 \pm 1.01) * 10^{-4}$ $P_{ref} = 220 \text{ MPa}$ $T_{ref} = 293 \text{ K}$	SAS	(Reyns et al., 2000)

Table 6. Reported parameters for the secondary Hawley thermodynamic model and its variants.

Target	Medium	Pressure Come Up Time Holding time Depressurization Temperature	Kinetic model	Model parameters	Regression software	Reference
Chymotrypsinogen	Aqueous solution, pH 2.07	0.1-700 MPa NR NR NR 8.5-70°C	Thermodynamic model (Eq. 73)	$\Delta\beta = -0.296 \text{ cm}^6 \text{ J}^{-1} \text{ mol}^{-1}$ $\Delta V_{ref}^\ddagger = -14.3 \text{ cm}^3 \text{ mol}^{-1}$ $\Delta S_{ref} = 950 \text{ J mol}^{-1} \text{ K}^{-1}$ $\Delta\alpha = 1.32 \text{ cm}^3 \text{ mol}^{-1} \text{ K}^{-1}$ $\Delta C_p = 15,900 \text{ J mol}^{-1}$ $*\ln k_{ref} = -4.66$ $P_{ref} = 0.1 \text{ MPa}$ $T_{ref} = 273 \text{ K}$ $*\text{Calculated from reported } \Delta G^0$	NR	(Hawley, 1971)

Lipoxygenase (LOX)	Green pea juice	0.1-625 MPa 100-125 MPa min ⁻¹ 0.1-625 MPa NR (-15)-70°C	Thermodynamic model (Eq. 75)	$\Delta\beta = -(0.0937 \pm 0.0192) \text{ cm}^6 \text{ J}^{-1} \text{ mol}^{-1}$ $\Delta V_{ref}^\ddagger = -(38.18 \pm 3.37) \text{ cm}^3 \text{ mol}^{-1}$ $\Delta S_{ref} = 13.79 \pm 11.78 \text{ J mol}^{-1} \text{ K}^{-1}$ $\Delta\alpha = -(0.12 \pm 0.09) \text{ cm}^3 \text{ mol}^{-1} \text{ K}^{-1}$ $\Delta C_p = 1,837.4 \pm 244.0 \text{ J mol}^{-1}$ $\ln k_{ref} = -3.71$ $P_{ref} = 500 \text{ MPa}$ $T_{ref} = 298 \text{ K}$	SAS	(Indrawati et al., 2001)
Lipoxygenase (LOX)	Green pea	0.1-625 MPa 100-125 MPa min ⁻¹ 0.1-625 MPa NR (-10)-70°C	Thermodynamic model (Eq. 75)	$\Delta\beta = -(0.1382 \pm 0.0406) \text{ cm}^6 \text{ J}^{-1} \text{ mol}^{-1}$ $\Delta V_{ref}^\ddagger = -(50.76 \pm 7.37) \text{ cm}^3 \text{ mol}^{-1}$ $\Delta S_{ref} = 21.19 \pm 25.69 \text{ J mol}^{-1} \text{ K}^{-1}$ $\Delta\alpha = -(0.23 \pm 0.20) \text{ cm}^3 \text{ mol}^{-1} \text{ K}^{-1}$ $\Delta C_p = 1,058.6 \pm 375.0 \text{ J mol}^{-1}$ $\ln k_{ref} = -2.85$ $P_{ref} = 500 \text{ MPa}$ $T_{ref} = 298 \text{ K}$	SAS	(Indrawati et al., 2001)

Lipoxygenase (LOX)	Tris-HCl buffer	0.1-625 MPa	Thermodynamic model (Eq. 75)	$\Delta\beta = -(0.1382 \pm 0.0406) \text{ cm}^6 \text{ J}^{-1} \text{ mol}^{-1}$ $\Delta V_{ref}^\ddagger = -(50.76 \pm 7.37) \text{ cm}^3 \text{ mol}^{-1}$ $\Delta S_{ref} = 21.19 \pm 25.69 \text{ J mol}^{-1} \text{ K}^{-1}$ $\Delta\alpha = -(0.23 \pm 0.20) \text{ cm}^3 \text{ mol}^{-1} \text{ K}^{-1}$ $\Delta C_p = 1,058.6 \pm 375.0 \text{ J mol}^{-1}$ $\ln k_{ref} = -2.85$ $P_{ref} = 0.5 \text{ MPa}$ $T_{ref} = 298 \text{ K}$	SAS	(Indrawati et al., 1999)
	0.1 M, pH 9	100-125 MPa min ⁻¹				
	Lyophilized soybean LOX powder	0.1-625 MPa				
	NR	NR				
	0.4 mg enzyme powder per ml of buffer	(-10)-70°C				
Pectinmethylesterase (PME)	Tris-HCl buffer	100-825 MPa	Thermodynamic model (Eq. 75)	$\Delta\beta = -(1.40 \pm 1.06) \text{ cm}^6 \text{ J}^{-1} \text{ mol}^{-1}$ $\Delta V_{ref}^\ddagger = -(341.95 \pm 22.21) \text{ cm}^3 \text{ mol}^{-1}$ $\Delta S_{ref} = -20.65 \pm 7.20 \text{ J mol}^{-1} \text{ K}^{-1}$ $\Delta\alpha = 3.20 \pm 0.26 \text{ cm}^3 \text{ mol}^{-1} \text{ K}^{-1}$ $\Delta C_p = 3,046.6 \pm 207.2 \text{ J mol}^{-1}$ $\ln k_{ref} = -4.36$ $P_{ref} = 700 \text{ MPa}$ $T_{ref} = 323 \text{ K}$	NR	(Ly-Nguyen et al., 2003)
	20 mM, pH 7.0	100 MPa min ⁻¹				
	Carrot PME extract	0-250 min				
	NR	NR				
	NR	10-65°C				

Pectinmethylesterase (PME)	Tris-HCl buffer 20 mM, pH 7.0 Carrot PME extract	100-825 MPa 100 MPa min ⁻¹ 0-250 min NR 10-65°C	Extended thermodynamic model (Eq. 76-77)	$\Delta\beta = -(0.0307 \pm 0.03467) \text{ cm}^6 \text{ J}^{-1} \text{ mol}^{-1}$ $\Delta V_{ref}^\ddagger = -(41.64 \pm 2.70) \text{ cm}^3 \text{ mol}^{-1}$ $\Delta S_{ref} = 148.3 \pm 24.01 \text{ J mol}^{-1} \text{ K}^{-1}$ $\Delta\alpha = -(0.0415 \pm 0.0967) \text{ cm}^3 \text{ mol}^{-1} \text{ K}^{-1}$ $\Delta C_p = 4,573.9 \pm 1306.7 \text{ J mol}^{-1}$ $\ln k_{ref} = -2.70$ $\Delta\beta_2 = -(0.00012 \pm 0.00004) [\text{cm}^6 \text{ J}^{-1} \text{ mol}^{-1}]^2$ $\Delta\alpha_2 = 0.00026 \pm 0.00015 [\text{cm}^3 \text{ mol}^{-1} \text{ K}^{-1}]^2$ $\Delta C_{p2} = 88.02 \pm 28.94 [\text{J mol}^{-1}]^2$ $P_{ref} = 700 \text{ MPa}$ $T_{ref} = 323 \text{ K}$	NR	(Ly-Nguyen et al., 2003)
Polygalacturonase (PG)	Sodium acetate buffer 40 mM, pH 4.4 Tomato PG extract	300-600 MPa 100 MPa min ⁻¹ 0-200 min NR 5-50°C	Reduced thermodynamic model (Eq. 78)	$\Delta V_{ref}^\ddagger = -(55.69 \pm 2.95) \text{ cm}^3 \text{ mol}^{-1}$ $\Delta S_{ref} = 265.28 \pm 18.14 \text{ J mol}^{-1} \text{ K}^{-1}$ $\Delta\alpha = -(1.029 \pm 0.15) \text{ cm}^3 \text{ mol}^{-1} \text{ K}^{-1}$ $\ln k_{ref} = -3.26$ $P_{ref} = 400 \text{ MPa}$ $T_{ref} = 298 \text{ K}$	SAS	(Fachin et al., 2002)

Table 7 Reported simultaneous effect of pressure and temperature on the Weibull model parameters that describe PATP kinetics.

Target	Medium	Pressure	Kinetic model	Model parameters	Regression software	Reference
		Come Up Time Holding time Depressurization Temperature				
<i>Escherichia coli</i>	Peptone water 0.1%, pH 6.95 10 ⁷ cfu ml ⁻¹ O157:H7 933 strain Stationary phase	200-400 MPa	Weibull parameter <i>n</i> inverse (Eq. 85)	$n_{ref} = 0.4 \pm 0.08$ $a = 125.5 \pm 10.2$ MPa	SigmaPlot 2000 v. 6.00	(Pilavtepe- Çelik et al., 2009)
		400 MPa min ⁻¹				
		5-40 min				
		>20 s				
<i>Escherichia coli</i>	Whey protein surrogate food system ATCC 11229 strain	207-439 MPa	Weibull (Eq. 80, 86)	$P_c = 357-458$ MPa (30-50°C) $w_p = 0.026-0.042$ 1/MPa (30- 50°C) $d_{0p} = 5.7-43.3$ (30-50°C) $d_{1p} = 0.00039-0.00077$ (30-50°C)	NR	(Doona et al., 2008)
		NR				
		0-300 min				
		NR				
<i>Lactobacillus plantarum</i>	Fresh clementine mandarin (<i>Citrus reticula</i> , variety <i>Nules</i>) juice 2x10 ⁸ cfu ml ⁻¹ inoculum	0-450 MPa	Pressure dependent Weibull biphasic model (Eq. 91)	$f_p = 128-335$ MPa (15-45°C) $n = 2.41-7.55$ (15-45°C)	Statgraphics Centurion XV	(Carreño et al., 2011)
		90 sec				
		10-60 sec				
		15 sec				
		15, 30, 45°C (initial)				

<i>Lactobacillus plantarum</i>	Mandarin juice	0-450 MPa	Pressure dependent Weibull biphasic model (Eq. 91)	$\Psi = 2.56-3.08$ (15-45°C)	Statgraphics Centurion XV	(Carreño et al., 2011)
	Clementine mandarin (<i>Citrus reticula</i> , commercial variety <i>Nules</i>)	90 s		$f_{P1} = 128-335$ MPa (15-45°C)		
	Fresh juice	10-60 s		$f_{P2} = 445-668$ MPa (15-45°C)		
	2×10^8 cfu ml ⁻¹ inoculum	15 s		$n = 3.28-6.00$ (15-45°C)		
<i>Staphylococcus aureus</i>	Carrot juice (pH 6.22)	200-400 MPa	Weibull parameter n inverse (Eq. 85)	$n_{ref} = 0.6 \pm 0.1$	SigmaPlot 2000 6.00	(Pilavtepe-Çelik et al., 2009)
	Fresh, squeezed juice	400 MPa min ⁻¹		$a = 230.4 \pm 65.4$ MPa		
	10^7 cfu ml ⁻¹	5-40 min				
	485 strain	>20 s				
<i>Staphylococcus aureus</i>	Stationary phase	40°C				
	Peptone water	200-400 MPa	Weibull parameter n inverse (Eq. 85)	$n_{ref} = 0.6 \pm 0.06$	SigmaPlot 2000 6.00	(Pilavtepe-Çelik et al., 2009)
	0.1%, pH 6.95	400 MPa min ⁻¹		$a = 332.5 \pm 50.1$ MPa		
	10^7 cfu ml ⁻¹	5-40 min				
485 strain	>20 s					
	Stationary phase	40°C				

References

- Ahn, J., Balasubramaniam, V.M., Yousef, A.E., (2007). Inactivation kinetics of selected aerobic and anaerobic bacterial spores by pressure-assisted thermal processing. *International Journal of Food Microbiology* 113(3), 321-329.
- Atkins, P., de Paula, J., (2006). *Atkins' Physical Chemistry* (8th Edition ed). Oxford University Press.
- Balasubramaniam, V.M., Farkas, D.F., Turek, E., (2008). Preserving foods through high-pressure processing. *Food Technology* 62(11), 32-38.
- Baranyi, J., Roberts, T.A., (1994). A dynamic approach to predicting bacterial growth in food. *International Journal of Food Microbiology* 23(3-4), 277-294.
- Barbosa-Cánovas, G.V., Juliano, P., (2008). Food Sterilization by Combining High Pressure and Thermal Energy, in: Gutiérrez-López, G.F., Barbosa-Cánovas, G.V., Welte-Chanes, J., Parada-Arias, E. (Eds.), *Food Engineering: Integrated Approaches*. Springer New York, pp. 9-46.
- Basak, S., Ramaswamy, H.S., Simpson, B.K., (2001). High Pressure Inactivation of Pectin Methyl Esterase in Orange Juice Using Combination Treatments. *Journal of Food Biochemistry* 25, 509-526.
- Bermúdez-Aguirre, D., Barbosa-Cánovas, G., (2011). An Update on High Hydrostatic Pressure, from the Laboratory to Industrial Applications. *Food Engineering Reviews* 3(1), 44-61.
- Bigelow, W.D., (1921). The logarithmic nature of thermal death time curves. *Journal of Infectious Diseases* 29 (5), 528-536.
- Borda, D., Van Loey, A., Smout, C., Hendrickx, M., (2004). Mathematical Models for Combined High Pressure and Thermal Plasmin Inactivation Kinetics in Two Model Systems. *Journal of Dairy Science* 87(12), 4042-4049.
- Buzrul, S., Alpas, H., (2004). Modeling the synergistic effect of high pressure and heat on inactivation kinetics of *Listeria innocua*: a preliminary study. *FEMS Microbiology Letters* 238(1), 29-36.
- Buzrul, S., Alpas, H., Largeteau, A., Demazeau, G., (2008). Modeling high pressure inactivation of *Escherichia coli* and *Listeria innocua* in whole milk. *European Food Research and Technology* 227(2), 443-448.
- Campanella, O.H., Peleg, M., (2001). Theoretical comparison of a new and the traditional method to calculate *Clostridium botulinum* survival during thermal inactivation. *Journal of the Science of Food and Agriculture* 81(11), 1069-1076.
- Carreño, J., Gurrea, M., Sampedro, F., Carbonell, J., (2011). Effect of high hydrostatic pressure and high-pressure homogenisation on *Lactobacillus plantarum* inactivation kinetics and quality parameters of mandarin juice. *European Food Research and Technology* 232(2), 265-274.
- Chen, C.S., Wu, M.C., (1998). Kinetic models for thermal inactivation of multiple pectinesterases in citrus juices. *Journal of Food Science* 63(5), 747-750.
- Chen, H., Hoover, D.G., (2003a). Pressure inactivation kinetics of *Yersinia enterocolitica* ATCC 35669. *International Journal of Food Microbiology* 87(1-2), 161-171.
- Chen, H., Hoover, D.G., (2003b). Pressure inactivation kinetics of *Yersinia enterocolitica* ATCC 35669. *International Journal of Food Microbiology* 87(1-2), 161-171.
- Chen, H., (2007). Use of linear, Weibull, and log-logistic functions to model pressure inactivation of seven foodborne pathogens in milk. *Food Microbiology* 24(3), 197-204.
- Clark, N.A., (1979). Thermodynamics of the Re-Entrant Nematic-Bilayer Smectic a Transition. *J. Phys. Colloques* 40(C3), C3-345-C343-349.

Cole, M.B., Davies, K.W., Munro, G., Holyoak, C.D., Kilsby, D.C., (1993). A vitalistic model to describe the thermal inactivation of *Listeria monocytogenes*. *Journal of Industrial Microbiology & Biotechnology* 12(3), 232-239.

Cook, D.W., (2003). Sensitivity of *Vibrio* Species in Phosphate-Buffered Saline and in Oysters to High-Pressure Processing. *Journal of Food Protection* 66(12), 2276-2282.

Coroller, L., Leguerinel, I., Mettler, E., Savy, N., Mafart, P., (2006). General Model, Based on Two Mixed Weibull Distributions of Bacterial Resistance, for Describing Various Shapes of Inactivation Curves. *Appl. Environ. Microbiol.* 72(10), 6493-6502.

Corradini, M.G., Normand, M.D., Peleg, M., (2005). Calculating the efficacy of heat sterilization processes. *Journal of Food Engineering* 67(1-2), 59-69.

Corradini, M.G., Normand, M.D., Newcomer, C., Schaffner, D.W., Peleg, M., (2009). Extracting Survival Parameters from Isothermal, Isobaric, and “Iso-concentration” Inactivation Experiments by the “3 End Points Method”. *Journal of Food Science* 74(1), R1-R11.

Cruz, R.M.S., Rubilar, J.F., Ulloa, P.A., Torres, J.A., Vieira, M.C., (2011). New food processing technologies: development and impact on the consumer acceptability, in: Columbus, F. (Ed.), *Food quality: Control, analysis and consumer concerns*. Nova Science Publishers, New York, NY, p. (In press).

Daek, T., Farkas, J., (2012). Thermal Destruction of Microorganisms, *Microbiology of Thermally Preserved Foods: Canning and Novel Physical Methods*. DEStech Publications Inc., pp. 105-160.

Daryaei, H., Balasubramaniam, V.M., (2013). Kinetics of *Bacillus coagulans* spore inactivation in tomato juice by combined pressure-heat treatment. *Food Control* 30(1), 168-175.

de Heij, W., van Scepdael, L., Moezelaar, R., Hoogland, H., Master, A.M., Van den Berg, R.W., (2003). High-Pressure Sterilization: Maximizing the Benefits of Adiabatic Heating. *Food Technology* 57(3), 37-41.

Denys, S., Van Loey, A.M., Hendrickx, M.E., (2000). A modeling approach for evaluating process uniformity during batch high hydrostatic pressure processing: combination of a numerical heat transfer model and enzyme inactivation kinetics. *Innovative Food Science & Emerging Technologies* 1(1), 5-19.

Dogan, C., Erkmen, O., (2004). High pressure inactivation kinetics of *Listeria monocytogenes* inactivation in broth, milk, and peach and orange juices. *Journal of Food Engineering* 62(1), 47-52.

Doona, C.J., Feeherry, F.E., Ross, E.W., (2005). A quasi-chemical model for the growth and death of microorganisms in foods by non-thermal and high-pressure processing. *International Journal of Food Microbiology* 100(1-3), 21-32.

Doona, C.J., Feeherry, F.E., Ross, E.W., Corradini, M., Peleg, M., (2008). The Quasi-Chemical and Weibull Distribution Models of Nonlinear Inactivation Kinetics of *Escherichia Coli* ATCC 11229 by High Pressure Processing, *High Pressure Processing of Foods*. Blackwell Publishing Ltd, pp. 115-144.

Doona, C.J., Feeherry, F.E., Ross, E.W., Kustin, K., (2012). Inactivation Kinetics of *Listeria monocytogenes* by High-Pressure Processing: Pressure and Temperature Variation. *Journal of Food Science* 77(8), M458-M465.

Eisenmenger, M.J., Reyes-De-Corcuera, J.I., (2009). High pressure enhancement of enzymes: A review. *Enzyme and Microbial Technology* 45(5), 331-347.

Fachin, D., Loey, A.V., VanLoeyIndrawati, A., Ludikhuyze, L., Hendrickx, M., (2002). Thermal and High-Pressure Inactivation of Tomato Polygalacturonase: A Kinetic Study. *Journal of Food Science* 67(5), 1610-1615.

Farkas, D.F., Hoover, D.G., (2000). High pressure processing. *Journal of Food Safety* 65, 47-64.

Ghawi, S.K., Methven, L., Rastall, R.A., Niranjana, K., (2012). Thermal and high hydrostatic pressure inactivation of myrosinase from green cabbage: A kinetic study. *Food Chemistry* 131(4), 1240-1247.

Grauwet, T., Plancken, I.V.d., Vervoort, L., Hendrickx, M.E., Loey, A.V., (2010). Protein-based indicator system for detection of temperature differences in high pressure high temperature processing. *Food Research International* 43(3), 862-871.

Guan, D., Chen, H., Hoover, D.G., (2005). Inactivation of *Salmonella typhimurium* DT 104 in UHT whole milk by high hydrostatic pressure. *International Journal of Food Microbiology* 104(2), 145-153.

Guan, D., Chen, H., Ting, E.Y., Hoover, D.G., (2006). Inactivation of *Staphylococcus aureus* and *Escherichia coli* O157:H7 under isothermal-endpoint pressure conditions. *Journal of Food Engineering* 77(3), 620-627.

Hartmann, C., Delgado, A., (2002). Numerical simulation of convective and diffusive transport effects on a high-pressure-induced inactivation process. *Biotechnology and Bioengineering* 79(1), 94-104.

Hartmann, C., Delgado, A., (2003). The influence of transport phenomena during high-pressure processing of packed food on the uniformity of enzyme inactivation. *Biotechnology and Bioengineering* 82(6), 725-735.

Hashizume, C., Kimura, K., Hayashi, R., (1995). Kinetic Analysis of Yeast Inactivation by High Pressure Treatment at Low Temperatures. *Bioscience, Biotechnology, and Biochemistry* 59(8), 1455-1458.

Hawley, S.A., (1971). Reversible pressure-temperature denaturation of chymotrypsinogen. *Biochemistry* 10(13), 2436-2442.

Heremans, K., (1982). High Pressure Effects on Proteins and other Biomolecules. *Annual Review of Biophysics & Bioengineering* 11(1), 1-21.

Heremans, K., Smeller, L., (1998). Protein structure and dynamics at high pressure. *Biochimica et Biophysica Acta (BBA) - Protein Structure and Molecular Enzymology* 1386(2), 353-370.

Holdsworth, D., Simpson, R., (2007). Kinetics of Thermal Processing, *Thermal Processing of Packaged Foods*. Springer US, pp. 87-122.

House, J.E., (2007). Techniques and Methods, in: House, J.E. (Ed.), *Principles of Chemical Kinetics*, 2^o ed, pp. 79-109.

Indrawati, Van Loey, A.M., Ludikhuyze, L.R., Hendrickx, M.E., (1999). Soybean Lipoyxygenase Inactivation by Pressure at Subzero and Elevated Temperatures. *Journal of Agricultural and Food Chemistry* 47(6), 2468-2474.

Indrawati, I., Van Loey, A., Ludikhuyze, L., Hendrickx, M., (2001). Pressure-temperature inactivation of lipoyxygenase in green peas (*Pisum sativum*): A kinetic study. *Journal of Food Science* 66(5), 686-693.

Infante, J.A., Ivorra, B., Ramos, Á.M., Rey, J.M., (2009). On the Modelling and Simulation of High Pressure Processes and Inactivation of Enzymes in Food Engineering. *Mathematical Models and Methods in Applied Sciences* 19(12), 2203-2229.

Isaacs, N.S., (1981). Effects of Pressure on Rate Processes, in: Isaacs, N.S. (Ed.), *Liquid Phase High Pressure Chemistry*, 1^o ed. Wiley-Interscience, pp. 181-352.

Katsaros, G.I., Tsevdou, M., Panagiotou, T., Taoukis, P.S., (2010). Kinetic study of high pressure microbial and enzyme inactivation and selection of pasteurisation conditions for Valencia Orange Juice. *International Journal of Food Science & Technology* 45(6), 1119-1129.

Kingsley, D.H., Holliman, D.R., Calci, K.R., Chen, H., Flick, G.J., (2007). Inactivation of a Norovirus by High-Pressure Processing. *Applied and Environmental Microbiology* 73(2), 581-585.

Knoerzer, K., Juliano, P., Roupas, P., Versteeg, C., (2011). *Innovative Food Processing Technologies: Advances in Multiphysics Simulation*. Blackwell Publishing Ltd.

Koo, J., Jahncke, M.L., Reno, P.W., Hu, X., Mallikarjunan, P., (2006). Inactivation of *Vibrio parahaemolyticus* and *Vibrio vulnificus* in phosphate-buffered saline and in inoculated whole oysters by high-pressure processing. *Journal of Food Protection* 69(3), 596-601.

Koseki, S., Yamamoto, K., (2007). A novel approach to predicting microbial inactivation kinetics during high pressure processing. *International Journal of Food Microbiology* 116(2), 275-282.

Lado, B.H., Yousef, A.E., (2002). Alternative food-preservation technologies: efficacy and mechanisms. *Microbes and Infection* 4, 433-440.

Leskovac, V., (2003). Chemical Kinetics, *Comprehensive Enzyme Kinetics*. Kluwer Academics/Plenum Publishers, pp. 11-30.

López-Gómez, A., Fernández, P., Palop, A., Periago, P., Martínez-López, A., Marin-Iniesta, F., Barbosa-Cánovas, G., (2009). Food Safety Engineering: An Emergent Perspective. *Food Engineering Reviews* 1(1), 84-104.

Ludikhuyze, L., Indrawati, Van den Broeck, I., Weemaes, C., Hendrickx, M., (1998a). Effect of Combined Pressure and Temperature on Soybean Lipooxygenase. 2. Modeling Inactivation Kinetics under Static and Dynamic Conditions. *Journal of Agricultural and Food Chemistry* 46(10), 4081-4086.

Ludikhuyze, L., Indrawati, Van den Broeck, I., Weemaes, C., Hendrickx, M., (1998b). Effect of Combined Pressure and Temperature on Soybean Lipooxygenase. 1. Influence of Extrinsic and Intrinsic Factors on Isobaric–Isothermal Inactivation Kinetics. *Journal of Agricultural and Food Chemistry* 46(10), 4074-4080.

Ludikhuyze, L., Claeys, W., Hendrickx, M., (2000). Combined Pressure—temperature Inactivation of Alkaline Phosphatase in Bovine Milk: A Kinetic Study. *Journal of Food Science* 65(1), 155-160.

Ludikhuyze, L., Loey, A., Denys, I.S., Hendrickx, M.E.G., (2002). Effects of High Pressure on Enzymes Related to Food Quality, in: Hendrickx, M.E.G., Knorr, D., Ludikhuyze, L., Loey, A., Heinz, V. (Eds.), *Ultra High Pressure Treatments of Foods*. Springer US, pp. 115-166.

Ludikhuyze, L.R., Van den Broeck, I., Weemaes, C.A., Hendrickx, M.E., (1997a). Kinetic Parameters for Pressure–Temperature Inactivation of *Bacillus subtilis* α -Amylase under Dynamic Conditions. *Biotechnology Progress* 13(5), 617-623.

Ludikhuyze, L.R., Van den Broeck, I., Weemaes, C.A., Herremans, C.H., Van Impe, J.F., Hendrickx, M.E., Tobback, P.P., (1997b). Kinetics for Isobaric–Isothermal Inactivation of *Bacillus subtilis* α -Amylase. *Biotechnology Progress* 13(5), 532-538.

Ly-Nguyen, B., Van Loey, A.M., Smout, C., ErenÖzcan, S., Fachin, D., Verlent, I., Truong, S.V., Duvetter, T., Hendrickx, M.E., (2003). Mild-Heat and High-Pressure Inactivation of Carrot Pectin Methyltransferase: A Kinetic Study. *Journal of Food Science* 68(4), 1377-1383.

Mafart, P., Couvert, O., Gaillard, S., Leguerinel, I., (2002). On calculating sterility in thermal preservation methods: application of the Weibull frequency distribution model. *International Journal of Food Microbiology* 72(1-2), 107-113.

- Mañas, P., Pagán, R., (2005). Microbial inactivation by new technologies of food preservation. *Journal of Applied Microbiology* 98(6), 1387-1399.
- Meersman, F., Smeller, L., Heremans, K., (2006). Protein stability and dynamics in the pressure–temperature plane. *Biochimica et Biophysica Acta (BBA) - Proteins and Proteomics* 1764(3), 346-354.
- Missen, R.W., Mims, C.A., Saville, B.A., (1999). Fundamentals of Reaction Rates, *Introduction to Chemical Reaction Engineering and Kinetics*. John Wiley & Sons, Inc., pp. 115-153.
- Morales-Blancas, E.F., Torres, J.A., (2003a). Thermal resistance constant, *Encyclopedia of Agricultural, Food, and Biological Engineering*. Marcel Dekker, Inc, New York, pp. 1030-1037.
- Morales-Blancas, E.F., Torres, J.A., (2003b). Activation energy in thermal process calculations, *Encyclopedia of Agricultural, Food, and Biological Engineering*. Marcel Dekker, Inc, New York, pp. 1-4.
- Morild, E., (1981). The Theory of Pressure Effects on Enzymes, in: C.B. Anfinsen, J.T.E., Frederic, M.R. (Eds.), *Advances in Protein Chemistry*. Academic Press, pp. 93-166.
- Mújica-Paz, H., Valdez-Fragoso, A., Samson, C., Welti-Chanes, J., Torres, J., (2011). High-pressure processing technologies for the pasteurization and sterilization of foods. *Food and Bioprocess Technology* 4(6), 969-985.
- NCFST, (2009). NCFST receives regulatory acceptance of novel food sterilization process, <http://www.avure.com/archive/documents/Press-release/ncfst-receives-regulatory-acceptance-of-novel-food-sterilization-process.pdf>, last visited on
- Otero, L., Ramos, A.M., de Elvira, C., Sanz, P.D., (2007). A model to design high-pressure processes towards an uniform temperature distribution. *Journal of Food Engineering* 78(4), 1463-1470.
- Otero, L., Guignon, B., Aparicio, C., Sanz, P.D., (2010). Modeling thermophysical properties of food under high pressure. *Critical Reviews in Food Science and Nutrition* 50(4), 344-368.
- Palou, E., López-Malo, A., Barbosa-Cánovas, G., Swanson, B.G., (2007). High-pressure treatment in food preservation, in: Rahman, M.S. (Ed.), *Handbook of Food Preservation*, Second ed. CRC, pp. 815-853.
- Parish, M.E., (1998). High pressure inactivation of *Saccharomyces cerevisiae*, endogenous microflora and pectinmethylesterase in orange juice. *Journal of Food Safety* 18, 57-65.
- Patazca, E., Koutchma, T., Balasubramaniam, V.M., (2007). Quasi-adiabatic temperature increase during high pressure processing of selected foods. *Journal of Food Engineering* 80(1), 199-205.
- Patterson, M.F., (2005). Microbiology of pressure-treated foods. *Journal of Applied Microbiology* 98(6), 1400-1409.
- Patterson, M.F., Linton, M., (2009). "Pasteurización" de alimentos por altas presiones, *Nuevas tecnologías en la conservación y transformación de alimentos*. International Marketing & Communication, S.A., pp. 59-72.
- Peleg, M., Cole, M.B., (1998). Reinterpretation of Microbial Survival Curves. *Critical Reviews in Food Science and Nutrition* 38(5), 353-380.
- Peleg, M., Engel, R., Gonzalez-Martinez, C., Corradini, M.G., (2002). Non-Arrhenius and non-WLF kinetics in food systems. *Journal of the Science of Food and Agriculture* 82(12), 1346-1355.
- Peleg, M., Normand, M.D., Corradini, M.G., (2005). Generating microbial survival curves during thermal processing in real time. *Journal of Applied Microbiology* 98(2), 406-417.

- Peleg, M., (2006). *Advanced Quantitative Microbiology for Foods and Biosystems*. CRC Taylor & Francis.
- Peleg, M., Corradini, M.G., Normand, M.D., (2012). On Quantifying Nonthermal Effects on the Lethality of Pressure-Assisted Heat Preservation Processes. *Journal of Food Science* 77(1), R47-R56.
- Pérez, P.M.C., Aliaga, R.D., Reyes, S.D., López, M., A., (2007). Pressure Inactivation Kinetics of *Enterobacter sakazakii* in Infant Formula Milk. *Journal of Food Protection* 70(10), 2281-2289.
- Pilavtepe-Çelik, M., Buzrul, S., Alpas, H., Bozoğlu, F., (2009). Development of a new mathematical model for inactivation of *Escherichia coli* O157:H7 and *Staphylococcus aureus* by high hydrostatic pressure in carrot juice and peptone water. *Journal of Food Engineering* 90(3), 388-394.
- Polydera, A.C., Galanou, E., Stoforos, N.G., Taoukis, P.S., (2004). Inactivation kinetics of pectin methylesterase of greek Navel orange juice as a function of high hydrostatic pressure and temperature process conditions. *Journal of Food Engineering* 62(3), 291-298.
- Rajan, S., Pandrangi, S., Balasubramaniam, V.M., Yousef, A.E., (2006). Inactivation of *Bacillus stearothermophilus* spores in egg patties by pressure assisted thermal processing. *Lebensmittel-Wissenschaft-und-Technologie* 39(8), 844-851.
- Ramaswamy, H.S., Shao, Y., Zhu, S., (2010). High-pressure destruction kinetics of *Clostridium sporogenes* ATCC 11437 spores in milk at elevated quasi-isothermal conditions. *Journal of Food Engineering* 96(2), 249-257.
- Ramirez, R., Saraiva, J., Pérez Lamela, C., Torres, J., (2009). Reaction Kinetics Analysis of Chemical Changes in Pressure-Assisted Thermal Processing. *Food Engineering Reviews* 1(1), 16-30.
- Ramos, Á.M., Smith, N. (2009). Mathematical models in food Engineering In *Proceedings of the Conference Name* |, Conference Location|.
- Rauh, C., Baars, A., Delgado, A., (2009). Uniformity of enzyme inactivation in a short-time high-pressure process. *Journal of Food Engineering* 91(1), 154-163.
- Reineke, K., Mathys, A., Knorr, D., (2011). The Impact of High Pressure and Temperature on Bacterial Spores: Inactivation Mechanisms of *Bacillus subtilis* above 500 MPa. *Journal of Food Science* 76(3), M189-M197.
- Reyns, K.M.F.A., Soontjens, C.C.F., Cornelis, K., Weemaes, C.A., Hendrickx, M.E., Michiels, C.W., (2000). Kinetic analysis and modelling of combined high-pressure–temperature inactivation of the yeast *Zygosaccharomyces bailii*. *International Journal of Food Microbiology* 56(2–3), 199-210.
- Ross, E.W., Taub, I.A., Doona, C.J., Feeherry, F.E., Kustin, K., (2005). The mathematical properties of the quasi-chemical model for microorganism growth–death kinetics in foods. *International Journal of Food Microbiology* 99(2), 157-171.
- Santillana Farakos, S., M., Zwietering, M.H., (2011). Data Analysis of the Inactivation of Foodborne Microorganisms under High Hydrostatic Pressure To Establish Global Kinetic Parameters and Influencing Factors. *Journal of Food Protection* 74(12), 2097-2106.
- Saucedo-Reyes, D., Marco-Celdrán, A., Pina-Pérez, M.C., Rodrigo, D., Martínez-López, A., (2009). Modeling survival of high hydrostatic pressure treated stationary- and exponential-phase *Listeria innocua* cells. *Innovative Food Science & Emerging Technologies* 10(2), 135-141.
- Segovia Bravo, K., Ramírez, R., Durst, R., Escobedo-Avellaneda, Z.J., Welti-Chanes, J., Sanz, P.D., Torres, J.A., (2012). Formation Risk of Toxic and Other

Unwanted Compounds in Pressure-Assisted Thermally Processed Foods. *Journal of Food Science* 77(1), R1-R10.

Shao, Y., Zhu, S., Ramaswamy, H., Marcotte, M., (2010). Compression Heating and Temperature Control for High-Pressure Destruction of Bacterial Spores: An Experimental Method for Kinetics Evaluation. *Food and Bioprocess Technology* 3(1), 71-78.

Smeller, L., (2002). Pressure–temperature phase diagrams of biomolecules. *Biochimica et Biophysica Acta (BBA) - Protein Structure and Molecular Enzymology* 1595(1–2), 11-29.

Smith, J.M., Van Ness, H.C., Abbot, M.M., (1997). *Introducción a la termodinámica en ingeniería química* (5° ed). McGraw Hill.

Toledo, R.T., (2007). *Fundamentals of Food Process Engineering* (Third ed). Springer, Athens, Georgia.

Torres, J.A., Velazquez, G., (2005). Commercial opportunities and research challenges in the high pressure processing of foods. *Journal of Food Engineering* 67(1-2), 95-112.

Torres, J.A., Sanz, P.D., Otero, L., Pérez Lamela, C., Saldaña, M.D.A., (2009). Temperature distribution and chemical reactions in foods treated by pressure-assisted thermal processing, in: Ortega-Rivas, E. (Ed.), *Processing effects on safety and quality of foods*. CRC Taylor & Francis, Inc., Boca Raton, FL, pp. 415-440.

Valdez-Fragoso, A., Mújica-Paz, H., Welti-Chanes, J., Torres, J., (2011). Reaction Kinetics at High Pressure and Temperature: Effects on Milk Flavor Volatiles and on Chemical Compounds with Nutritional and Safety Importance in Several Foods. *Food and Bioprocess Technology* 4(6), 986-995.

van Asselt, E.D., Zwietering, M.H., (2006). A systematic approach to determine global thermal inactivation parameters for various food pathogens. *International Journal of Food Microbiology* 107(1), 73-82.

van Boekel, M.A.J.S., (2002). On the use of the Weibull model to describe thermal inactivation of microbial vegetative cells. *International Journal of Food Microbiology* 74(1-2), 139-159.

van Boekel, M.A.J.S., (2008). Kinetic modeling of food quality: a critical review. *Comprehensive Reviews in Food Science and Food Safety* 7(1), 144-158.

Van den Broeck, I., Ludikhuyze, L.R., Van Loey, A.M., Hendrickx, M.E., (2000). Inactivation of orange pectinesterase by combined high-pressure and temperature treatments: a kinetic study. *Journal of Agricultural and Food Chemistry* 48(5), 1960-1970.

Van Eldik, R., Asano, T., Le Noble, W.J., (1989). Activation and reaction volumes in solution. 2. *Chemical Reviews* 89(3), 549-688.

Van Opstal, I., Vanmuysen, S.C.M., Wuytack, E.Y., Masschalck, B., Michiels, C.W., (2005). Inactivation of *Escherichia coli* by high hydrostatic pressure at different temperatures in buffer and carrot juice. *International Journal of Food Microbiology* 98(2), 179-191.

Van Scepdael, L., De Heij, W., Hoogland, H., (2004). Method for High Pressure Preservation, *United States Patent Application Publication*, p. 26.

Vega-Gálvez, A., Giovagnoli, C., Pérez-Won, M., Reyes, J.E., Vergara, J., Miranda, M., Uribe, E., Di Scala, K., (2012). Application of high hydrostatic pressure to aloe vera (*Aloe barbadensis* Miller) gel: Microbial inactivation and evaluation of quality parameters. *Innovative Food Science & Emerging Technologies* 13, 57–63.

- Velazquez, G., Vázquez, P., Vázquez, M., Torres, J.A., (2005). Avances en el procesado de alimentos por alta presión *Ciencia y Tecnología Alimentaria* 4(005), 353-367.
- Verlinde, P.H.C.J., Oey, I., Deborggraeve, W.M., Hendrickx, M.E., Van Loey, A.M., (2009). Mechanism and Related Kinetics of 5-Methyltetrahydrofolic Acid Degradation during Combined High Hydrostatic Pressure–Thermal Treatments. *Journal of Agricultural and Food Chemistry* 57(15), 6803-6814.
- Wang, B.-S., Li, B.-S., Zeng, Q.-X., Huang, J., Ruan, Z., Zhu, Z.-W., Li, L.I.N., (2009). Inactivation Kinetics and Reduction of *Bacillus Coagulans* Spore by the combination of High Pressure and Moderate Heat. *Journal of Food Process Engineering* 32(5), 692-708.
- Weemaes, C.A., Ludikhuyze, L.R., Van den Broeck, I., Hendrickx, M.E., (1998a). Effect of pH on Pressure and Thermal Inactivation of Avocado Polyphenol Oxidase: A Kinetic Study. *Journal of Agricultural and Food Chemistry* 46(7), 2785-2792.
- Weemaes, C.A., Ludikhuyze, L.R., Van den Broeck, I., Hendrickx, M.E., (1998b). Kinetics of combined pressure-temperature inactivation of avocado polyphenoloxidase. *Biotechnology and Bioengineering* 60(3), 292-300.
- Welti-Chanes, J., Barbosa-Cánovas, G., Aguilera, J.M., (2002). *Engineering and food for the 21st century*. CRC Press.
- Welti-Chanes, J., Martín-González, F., Guerrero-Beltrán, J.A., Barbosa-Cánovas, G., (2006). Water and biological structures at high-pressure, in: Buera, M.P., Welti-Chanes, J., Lillford, P.J., Corti, H.T. (Eds.), *Water Properties, Pharmaceutical, and Biological Materials*. CRC, pp. 205-231.
- Wilson, D.R., Dabrowski, L., Stringer, S., Moezelaar, R., Brocklehurst, T.F., (2008). High pressure in combination with elevated temperature as a method for the sterilisation of food. *Trends in Food Science & Technology* 19(6), 289-299.
- Yaldagard, M., Mortazavi, S.A., Tabatabaie, F., (2008). The principles of ultra high pressure technology and its application in food processing/preservation: a review of microbiological and quality aspects *African Journal of Biotechnology* 7(16), 2739-2767.
- Zhou, L., Zhang, Y., Hu, X., Liao, X., He, J., (2009). Comparison of the inactivation kinetics of pectin methylesterases from carrot and peach by high-pressure carbon dioxide. *Food Chemistry* 115(2), 449-455.

List of Figures

1. Influence of the Weibull model parameters on the shape of the microbial survival curve: (a) shape parameter n ; (b) scale parameter, b' .
2. Influence of Weibull biphasic model parameters on the shape of the microbial survival curve.
3. Log-logistic inactivation curve modeling for *Yersinia enterocolitica* survival in sodium phosphate buffer (0.1 M, pH 7) at 450 MPa and room temperature. Modified from Chen and Hoover (2003).
4. Sub-version of the Enhanced Quasi Chemical Kinetic Model (EQCKM) scheme describing microbial inactivation under high pressure; (M) microbial cells in lag phase; (M^*) metabolically active microbial cells in the growth phase; (BR) baroresistant microbial population; (D) dead microbial cells. Modified from Doona et al. (2012).
5. Experimental (symbols) and predicted (lines) inactivation rate constants of orange juice PME inactivation with the Eyring-Arrhenius model. Data reported by: (a) Plot generated from Katsaros et al. (2010); (b) Modified from Polydera et al. (2004).
6. Pressure-temperature isorate inactivation constant contour plots for PME extracted from orange and suspended in citric acid buffer (5 mM, pH 3.7). Modified from Van den Broeck et al. (2000)
7. Experimental (EX) and predicted values of the kinetic rate constant (k) as a function of pressure and temperature for carrot PME inactivation with the thermodynamic (TH; Eq. 76) and the extended thermodynamic model (ET; Eq. 76-77). Plots generated from Li-Nguyen et al. (2003).
8. Experimental (symbols) and predicted (lines) parameters of the Quasi Chemical Kinetic Model (QCKM) for *E. coli* inactivation at different pressure-temperature combinations: (a) inactivation rate constants (μ); (b) PATP times required to yield a 6 log reduction of *E. coli*. Modified from Doona et al. (2008).
9. Instantaneous microbial survival rate (Eq. 100) predicted by the dynamic Weibull inactivation model (Eq. 98). Modified from Peleg et al. (2005).
10. Schematic example of the HPP temperature profiles and population survival parameters required for the 3-endpoint method. Modified from Peleg et al. (2012).

List of Tables

1. Reported values for the first order inactivation kinetics and related models
2. Reported parameters for the primary Weibull model describing HPP inactivation kinetics.
3. Reported parameters for the primary log-logistic model describing HPP inactivation kinetics.
4. Reported parameters for an attempted global Bigelow secondary model. Modified from Santillana Farakos and Zwietering (2011).
5. Reported parameters for the secondary Eyring-Arrhenius model and its variants.
6. Reported parameters for the secondary Hawley thermodynamic model and its variants.
7. Simultaneous effect of pressure and temperature on the secondary Weibull model parameters that describe pressure and temperature effects.